SRI International

Final Report • February 1990

DATA ANALYSIS OF A TWO-LIDAR EXPERIMENT

John M. Livingston, Senior Research Meteorologist
Edward E. Uthe, Director
Atmospheric Science and Effects Program

SRI Project 4305

Prepared for:

U.S. Army Research Office
Attn: Dr. Walter A. Flood
Geosciences Division
P.O. Box 12211
Research Triangle Park, NC 27709-2211

Contract DAAL03-87-K-0146

333 Ravenswood Avenue • Menlo Park, CA 94025-3493 • (415) 326-6200 • FAX (415) 326-5512 • Telex 334486

Final Report • February 1990

DATA ANALYSIS OF A TWO-LIDAR EXPERIMENT

John M. Livingston, Senior Research Meteorologist
Edward E. Uthe, Director
Atmospheric Science and Effects Program

SRI Project 4305

Prepared for:

U.S. Army Research Office
Attn: Dr. Walter A. Flood
Geosciences Division
P.O. Box 12211
Research Triangle Park, NC 27709-2211

Contract DAAL03-87-K-0146

Approved:

Murray J. Baron, Director
Geoscience and Engineering Center

SRI International 333 Ravenswood Avenue • Menlo Park, CA 94025-3493 • (415) 326-6200 • FAX (415) 326-5512 • Telex 334486

UNCLASSIFIED
SECURITY CLASSIFICATION OF THIS PAGE

REPORT DOCUMENTATION PAGE

Form Approved OMB No. 0704-0188

1a. REPORT SECURITY CLASSIFICATION UNCLASSIFIED	1b. RESTRICTIVE MARKINGS N/A since Unclassified
2a. SECURITY CLASSIFICATION AUTHORITY N/A since Unclassified	3. DISTRIBUTION/AVAILABILITY OF REPORT
2b. DECLASSIFICATION/DOWNGRADING SCHEDULE N/A since Unclassified	
4. PERFORMING ORGANIZATION REPORT NUMBER(S) SRI Project 4305	5. MONITORING ORGANIZATION REPORT NUMBER(S) ARO 25628.1-GS
6a. NAME OF PERFORMING ORGANIZATION SRI International 6b. OFFICE SYMBOL (If applicable) GEC	7a. NAME OF MONITORING ORGANIZATION U.S. Army Research Office
6c. ADDRESS (City, State, and ZIP Code) 333 Ravenswood Avenue Menlo Park, California 94025	7b. ADDRESS (City, State, and ZIP Code) Geosciences Division P.O. Box 12211 Research Triangle Park, NC 27709-2211
8a. NAME OF FUNDING/SPONSORING ORGANIZATION 8b. OFFICE SYMBOL (If applicable)	9. PROCUREMENT INSTRUMENT IDENTIFICATION NUMBER DAAL03-87-K-0146
8c. ADDRESS (City, State, and ZIP Code)	10. SOURCE OF FUNDING NUMBERS PROGRAM ELEMENT NO. / PROJECT NO. / TASK NO / WORK UNIT ACCESSION NO.

11. TITLE (Include Security Classification)
DATA ANALYSIS OF A TWO-LIDAR EXPERIMENT

12. PERSONAL AUTHOR(S)
Livingston, John M. and Uthe, Edward E.

13a. TYPE OF REPORT	13b. TIME COVERED	14. DATE OF REPORT (Year, Month, Day)	15. PAGE COUNT
Final	FROM 09/87 TO 03/90	1990 February	52

16. SUPPLEMENTARY NOTATION

17. COSATI CODES			18. SUBJECT TERMS (Continue on reverse if necessary and identify by block number)	
FIELD	GROUP	SUB-GROUP		
			Lidar	Scattering
			Obscurants	Transmission
			Extinction	Lidar Solutions

19. ABSTRACT (Continue on reverse if necessary and identify by block number)

Lidar is a promising method for evaluating the optical and physical density distributions of obscurant clouds with high spatial and temporal resolution. However, single-lidar techniques may not completely penetrate dense obscurant clouds, and optical parameter assumptions necessary for inversion of lidar data can introduce unacceptable uncertainties in evaluated quantities. A two-lidar technique with each lidar observing the same optical path from opposite ends of the path may provide the means to quantitatively evaluate obscurant density parameters without the assumptions needed for analysis of single-lidar measurements.

To test the two-lidar technique, SRI International (SRI) operated two van-mounted 1.06-mm wavelength lidar systems at White Sands Missile Range (WSMR) during the period 6 through 18 May 1988 in conjunction with

20. DISTRIBUTION/AVAILABILITY OF ABSTRACT ☐ UNCLASSIFIED/UNLIMITED ☒ SAME AS RPT. ☐ DTIC USERS	21. ABSTRACT SECURITY CLASSIFICATION UNCLASSIFIED
22a. NAME OF RESPONSIBLE INDIVIDUAL Dr. Walter A. Flood	22b. TELEPHONE (Include Area Code) / 22c. OFFICE SYMBOL

DD Form 1473, JUN 86 *Previous editions are obsolete.*

the Characterization, Evaluation, and Comparison of Army Transmissometer Systems (CECATS) program. The two lidars were positioned at opposite ends of a near-common propagation path, and each laser path was terminated by a target with near-uniform reflection properties.

Comparisons of range-dependent backscattered signals confirm that both systems normally viewed the same obscurant density distributions along the near-common propagation path. Time-dependent values of the total path transmittance through the smoke were derived separately for the two lidar systems by analysis of the backscattered signals from the targets. These target-derived values of transmission were then utilized in the single-scattering lidar equation to calculate horizontal profiles of obscurant extinction. These results again illustrate the limitation of the single-lidar target method for deriving optical density profiles through dense obscurants.

Application of an analytical two-lidar inversion technique yielded unacceptable extinction retrievals -- namely, negative extinction coefficients over a significant portion of the laser propagation path. These results occurred regardless of the magnitude of the total path optical depth, or of the amount of signal smoothing employed in the analysis. To verify that the analysis algorithms were correct and to investigate reasons for the problems encountered, idealized lidar signatures were generated from single- and simple multiple-scattering formulations of the lidar equation, and these simulated signatures were processed by the two-lidar method. Results show that, when applied to the simulated signatures, the method produces excellent retrievals of the optical density profile used to simulate the lidar signatures. Therefore, the analysis method was correct and other reasons were investigated to explain the inability of this method to yield realistic optical density distributions.

Two possible reasons were identified that might account for the difficulties encountered in the application of the two-lidar inversion technique. The first is the performance of the extended-range logarithmic amplifiers that were installed within the lidar receivers specifically for acquiring data through dense obscurants. The second is the effect of multiple scattering on the emitted laser pulse length. In order to evaluate the first explanation, a detailed investigation of each lidar system response was undertaken. Analyses of the measurements in terms of lidar response functions and subsequent simulation of these responses in further modeling of the two-lidar inversion technique were performed. The results of these investigations indicate that small perturbations in the amplifier logarithmic response and/or amplifier saturation effects following observation of strong lidar returns can lead to large errors in two-lidar retrievals of optical density profiles. The expected effect of multiple scattering is to lengthen the laser pulse. However, no significant differences in signal decay were observed between backscattered target signals that were measured through clear air using attenuating optical neutral density filters and target returns of similar magnitudes measured through smoke. These results imply that it was the lidar receiver response problem, and not multiple scattering, that limited the effectiveness of the two-lidar method. It is concluded that improvement in the performance of the logarithmic amplifiers is necessary before the lidars can be used to evaluate the performance of the two-lidar technique.

CONTENTS

ILLUSTRATIONS

1. BACKGROUND AND SUMMARY

Improved measurement methods are needed to evaluate smoke/obscurant optical and physical densities along line-of-sight paths between electro-optical weapon and targeting systems and military targets. Such data are needed to assess the effectiveness of obscurant generation sources as countermeasures, as applied to various military scenarios and meteorological conditions. Lidar (laser radar) has been proposed as an attractive method to make the required measurements with extremely high spatial and temporal resolution. Several investigators have applied the lidar technique for dense obscurant evaluations with some degree of success [Evans, 1989; Uthe and Livingston, 1986; Uthe, 1981]. However, the full utility of the technique for this application has not been realized because of hardware and data interpretation problems.

The most basic problem is that the lidar signature is a function of more than one optical parameter, so that unique solutions for density distributions require assumptions for the optical parameters. Even for the case of a relatively low-density scattering aerosol volume, the lidar signature depends both on the backscatter coefficient at a given range and on the round-trip transmission of the laser energy between the lidar and the scattering volume. Several data interpretation methods are based on the single-scattering lidar (radar) equation and assumptions of backscatter-to-extinction ratios and boundary values at the near or far end of the observing path. While useful information can be obtained, unique obscurant densities that are highly reliable for a wide range of experimental conditions cannot be evaluated because of the inherent assumptions needed for signature analysis. This is especially true for dense obscurants because multiple scattering must be considered, and this requires even more assumptions on the nature of the scattering medium and instrumentation response characteristics. Other analysis methods have related features of the lidar signature (such as the path integrated signal) to optical depth and then used the resulting relationships to evaluate range-resolved extinction [Uthe and Livingston, 1986]. These methods account for multiple scattering but become insensitive to increased obscurant density for high density values. Clearly, the usefulness of the single-lidar technique is limited for quantitative evaluation of obscurant optical and/or physical densities along line-of-sight paths.

A two-lidar technique has been proposed [Kunz, 1987; Hughes and Paulson, 1988] as a method to overcome the inherent difficulties associated with data interpretation of the single-lidar technique. Basically, two lidars are used to observe nearly the same propagation path, but from opposite ends of the path. Then, because backscatter and extinction coefficients along the path are common to both lidars, the optical parameters can be evaluated uniquely from two-lidar measurements, providing the single-scattering lidar equation sufficiently represents the lidar signatures when applying true optical parameter values. Moreover, because unique single-scattering optical parameters can be evaluated, the technique

may provide a means to investigate multiple-scattering effects on laser energy propagation through dense aerosol volumes.

SRI International submitted a proposal to the Army Research Office (ARO) to investigate the usefulness of the two-lidar technique for evaluation of single- and multiple-scattering properties of obscurant distributions along propagation paths. The experiments were proposed to be conducted at SRI's Menlo Park lidar range facility. At about the time the work was awarded by ARO, the Office of the Project Manager Smokes/Obscurants (PM Smoke) planned to conduct a comprehensive evaluation of optical methods for obscurant measurements to be conducted at White Sands Missile Range (WSMR). ARO agreed to incorporate the two-lidar experiments into the CECATS (Characterization, Evaluation and Comparison of Army Transmissometer Systems) program, providing the additional data collection and analysis costs were provided by PM Smoke. The CECATS tests afforded the opportunity to observe a wide variety of obscurants, and also supplied corresponding data from independent sensors for further evaluation of the lidar method. PM Smoke provided SRI with specific data collection and data analysis tasks that assumed the two-lidar method would provide information anticipated in the proposal stage. The two-lidar experiments were conducted as part of CECATS. Early data analysis using single-lidar techniques indicated that good-quality data had been collected, and that evaluation of the two-lidar technique should proceed. However, further analysis indicated that although the two-lidar systems normally viewed the same obscurant density distributions along the near-common propagation path, the two-lidar signature analysis did not give results that could be considered correct, e.g. negative extinction coefficients. To verify that the analysis algorithms were correct and to investigate reasons for the problems encountered, idealized lidar signatures were generated from single- and multiple-scattering formulations of the lidar equation, and these simulated signatures were processed by the two-lidar method. Results showed that the two-lidar data analysis methods, when applied to the simulated signatures, resulted in excellent recovery of the optical density profile used to simulate lidar signatures. Therefore, it was concluded that the analysis method was correct and other reasons must be investigated for the inability to derive realistic optical density distributions from two-lidar measurements.

Two possible reasons for the two-lidar analysis difficulties were identified. The SRI lidar systems employ logarithmic amplifiers to process the 5 to 6 orders of magnitude of signal variation typically encountered during lidar observation of dense obscurants. During a series of previous experiments funded by ARO, it was demonstrated that signal strengths can vary over 5 orders of magnitude (50 dB) within 20 ns (3 meter) laser pulse propagation time. Extended dynamic-range amplifiers were installed within the lidar receivers specially for obscurant test evaluations, and were thought to provide sufficiently accurate signal processing for single-lidar evaluation of obscurant optical density evaluations [Uthe and Livingston, 1986). However, the amplifiers may satisfactorily process rapidly increasing lidar signals but not rapidly decreasing lidar signals if the amplifier has been driven into saturation. Because one of the

lidar signals of the two-lidar technique is always decreasing during the observation of an obscurant event, the two-lidar technique is very sensitive to the performance of the logarithmic amplifiers.

The other possible problem is that multiple scattering can lengthen the laser pulse and therefore cause a smoothing of the lidar signature. Therefore, the effect of multiple scattering is much like the effect of limited performance logarithmic amplifiers. Because we believe the two-lidar technique is the only possible lidar method for accurate evaluation of dense obscurant distributions, the effort of this program was directed to understanding the reason that the two-lidar technique did not provide anticipated results. Obviously, the original objective of applying the technique for evaluation of obscurant data for high-priority tests could not be achieved.

This report presents results from a series of data analysis tests to identify the reason the two-lidar methods did not perform as expected. It is concluded that the primary difficulty is the limited performance of the lidar logarithmic amplifiers and that this problem must be solved before the two-lidar technique can be evaluated for obscurant evaluations.

2. FIELD STUDY

During the period 6 through 18 May 1988, SRI International operated two van-mounted 1.06-μm wavelength lidar systems at White Sands Missile Range (WSMR) in conjunction with the Characterization, Evaluation, and Comparison of Army Transmissometer Systems (CECATS) test. The CECATS test was organized by the Project Manager for Smoke/Obscurants (PM Smoke) in order to characterize, evaluate, and compare transmissometer systems used in the U. S. Army smoke/obscurant test and evaluation programs. It has been described in detail in the CECATS Quick-Look Report (Farmer et al., 1988). The objective of the SRI research effort was twofold. The first goal was to demonstrate a method for making quantitative optical backscatter and extinction profile measurements through inhomogeneous aerosol clouds without the need for assumptions on the optical or physical parameter relationships that are typically needed to interpret optical signature data. The second objective was to develop methods that use the optical parameter measurements to evaluate the single-particle characteristics and multiple-scattering radiative transfer that govern propagation through dense obscurant clouds.

The two SRI lidars that were used during the CECATS test were the ALPHA 1 system, which was originally designed for use in the Electric Power Research Institute (EPRI) sponsored Plume Model Validation study and which, prior to CECATS, had been used in a variety of airborne plume and haze monitoring studies [Uthe, 1983], and the four-wavelength lidar system that was used during the Smoke Week VI and SNOW-TWO experiments [Uthe and Livingston, 1986]. Measurements were obtained at a wavelength of 1.06 μm only, a frequency of 5 pps, and a digitizer sampling interval of 10 ns, which corresponds to a range resolution of 1.5 m.

The CECATS test site and instrument configuration have been described in detail by Farmer et al. (1988). The SRI lidars were positioned at opposite ends of the test grid about 15 to 20 m east of the grid centerline, which was located along a near south-north (~345° with respect to true north) orientation. The propagation path of each lidar was terminated at a distance of approximately 1.9 km from the transmitter/receiver by a passive reflector target of near-uniform reflectivity. The locations of the lidars and their corresponding targets are shown in the horizontal plane and in a south-north vertical plane in Figure 2-1a and b, respectively. A solid line connecting the location of each lidar (designated by the letter A for the ALPHA 1 and B for the multiwavelength system) with the location of its corresponding target (T) is included to delineate the laser propagation path. The locations of the nephelometers (N) within one of the arrays operated by the U. S. Army Atmospheric Sciences Laboratory are shown for reference. The test grid center line is not shown, as it corresponds to a west coordinate of zero m (hence, off this scale) along the south-north direction.

The CECATS test period ran from 2 through 20 May 1988. The week of 2 through 6 May was used for setup and system debugging. On 6 May, interference tests between systems and a set of "no-data" trials were conducted. The first full operational test took place on 9 May. Data were obtained with the SRI lidars on the following dates: 6, 7, 10, 12, 16, 17, and 18 May.

During the analyses, several problems were encountered that prevented us from achieving our original study objectives. As a consequence, in this report we analyzed a much smaller volume of data than originally planned. Instead, we focus our discussion on explaining the results that were obtained. We detail the various methodologies used in the analyses, present the results of these analyses, and try to explain these results in the context of the difficulties encountered.

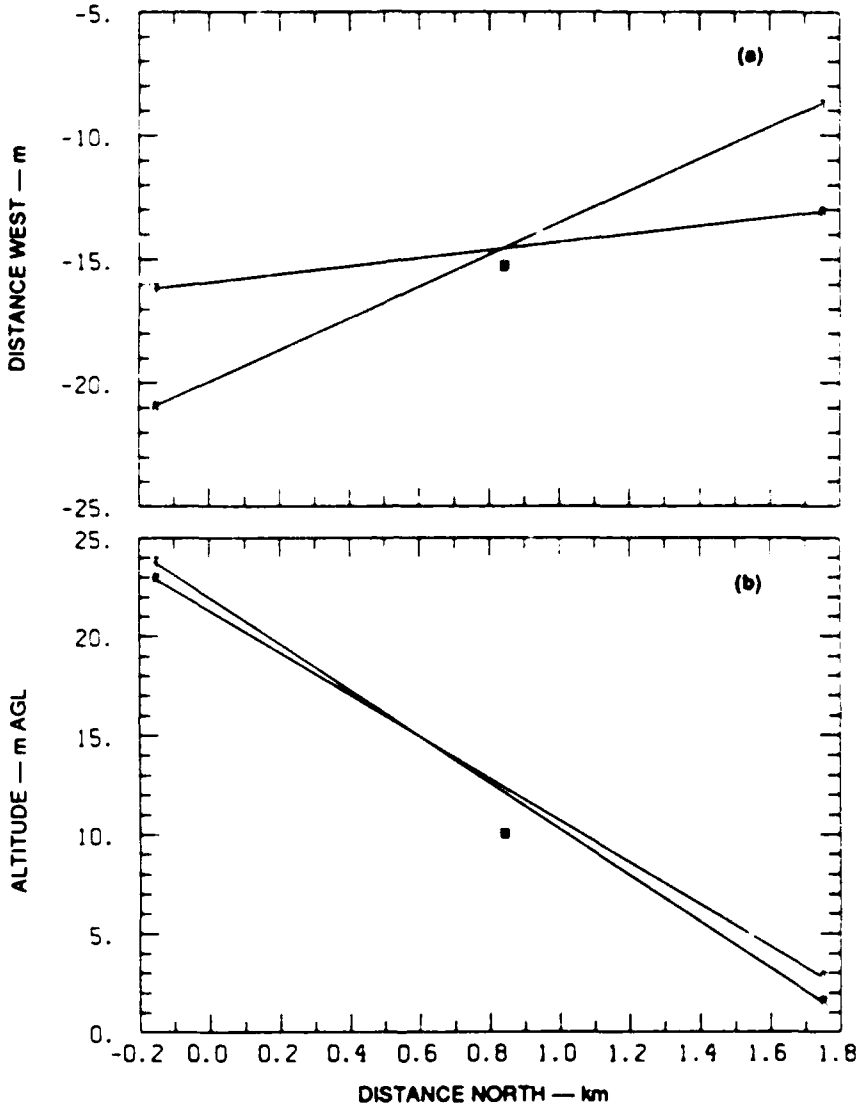

Figure 2-1. SRI two-lidar test grid configuration for CECATS Test. Each transmitter/receiver location is indicated by the letter R, with the corresponding target shown by the letter T. The letters N mark the locations of nephelometers within one array operated by the U.S. Army Atmospheric Sciences Laboratory.

3. LIDAR CALIBRATION

The backscattered signals measured by each lidar were logarithmically amplified, digitized at a sampling interval of 10 ns, and then stored on nine-track magnetic tape for subsequent analysis. For each lidar system, the response of the logarithmic amplifier was determined experimentally in terms of the number of recorded digitizer units (counts) per unit (dB) of signal attenuation. This calibration was performed in the following manner. First, a series of target measurements was taken during smoke-free atmospheric conditions, using optical filters of known optical density (separate analyses of the filters themselves were performed after CECATS by Melles Griot of Irvine, CA) to attenuate the backscattered signals. It was assumed that the atmosphere between the lidar and target was homogeneous during a particular calibration period. For each calibration test, the measured target returns were analyzed to determine means and standard deviations for each set of lidar shots that utilized a particular filter. Simple least-squares regression was then used to determine the optimum coefficients of a linear or quadratic function relating the magnitude of the measured target returns to the known magnitude of the signal attenuation introduced by use of the optical filters. Generally, this procedure was performed at least once per test day.

Figure 3-1 presents examples of digitized, logarithmically amplified backscatter signatures measured by each lidar under clear-air atmospheric conditions. Signals are shown as a function of time from the start of digitization. In general, both traces exhibit the familiar inverse range-squared dependence and are dominated by the large signal return from the respective targets, which were located approximately 1.9 km from the lidars. The slope difference between the two traces at digitization times before 1.5 μs is attributed to the different transmitter/receiver beam overlap functions between the two lidar systems. Clearly, the ALPHA 1 does not achieve complete overlap as soon as the multiwavelength system, as the ALPHA 1 trace does not exhibit the expected range-squared dependence before 1.5 μs. The smaller spikes at around 6 and 9.5 μs on the multiwavelength lidar trace are attributed to backscattering from wires that intersected the propagation path. Figure 3-2 shows time (record) dependent target returns from each lidar for one smoke test, trial 134b. The calibration data appear as decreases in the measured target returns prior to the smoke release.

Results of analysis of data obtained during individual calibration runs during CECATS are shown in Figure 3-3 for both lidar systems. Data for a particular run do not depart significantly from a straight line, as indicated by the correlation coefficients and least squares slopes listed in Table 3-1. Hence, the best-fit lines to the composite data sets are shown in Figure 3-3, and the corresponding slopes are used in the subsequent analysis. In particular, these values are 3.186 ± 0.080 cts/dB (0.314 dB/ct) for the ALPHA 1 system, and 3.758 ± 0.064 cts/dB (0.266 dB/ct) for the multiwavelength system.

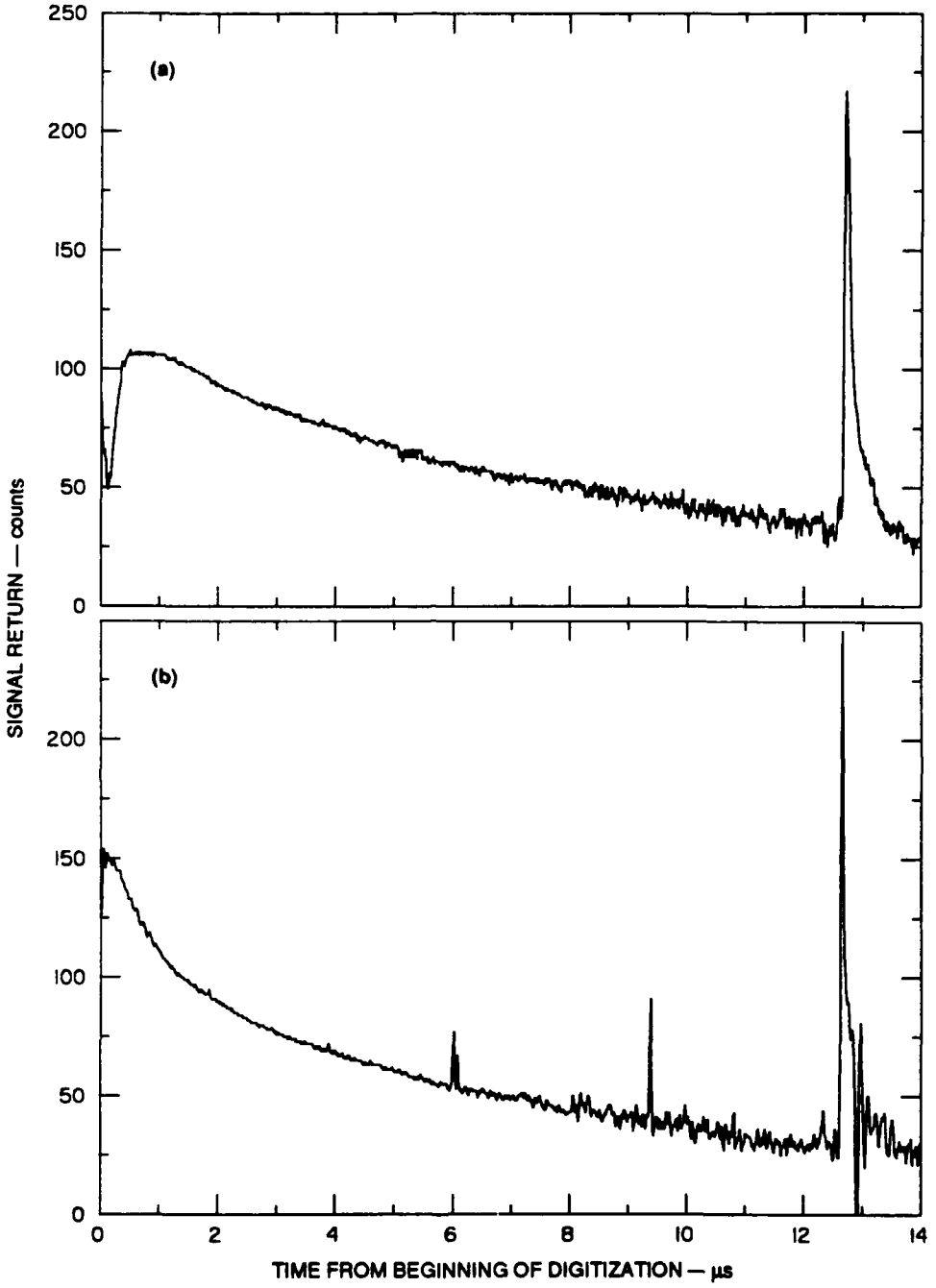

Figure 3-1. Digitized backscattered signals measured through clear air during CECATS by the SRI lidars: (a) ALPHA 1 system, and (b) multiwavelength system. For each system, the sharp peak between 12 and 13 μs is due to backscattering from the target.

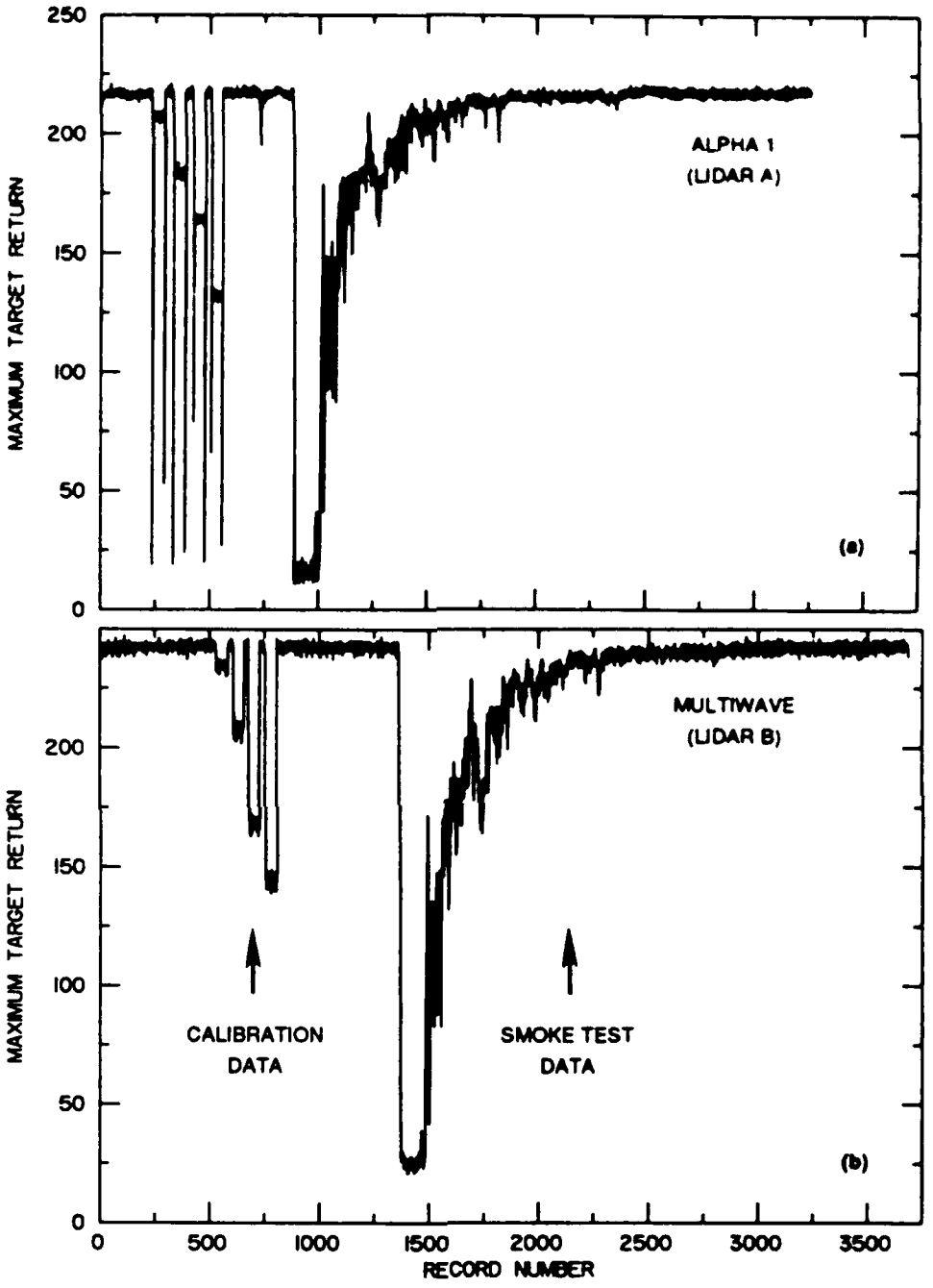

Figure 3-2. Measured target returns as a function of lidar shot (record) number for CECATS trial 134b: (a) ALPHA 1 lidar, and (b) multiwavelength lidar. The absolute time scales (not shown) differ for the two traces, but the total elapsed time is about 12 minutes.

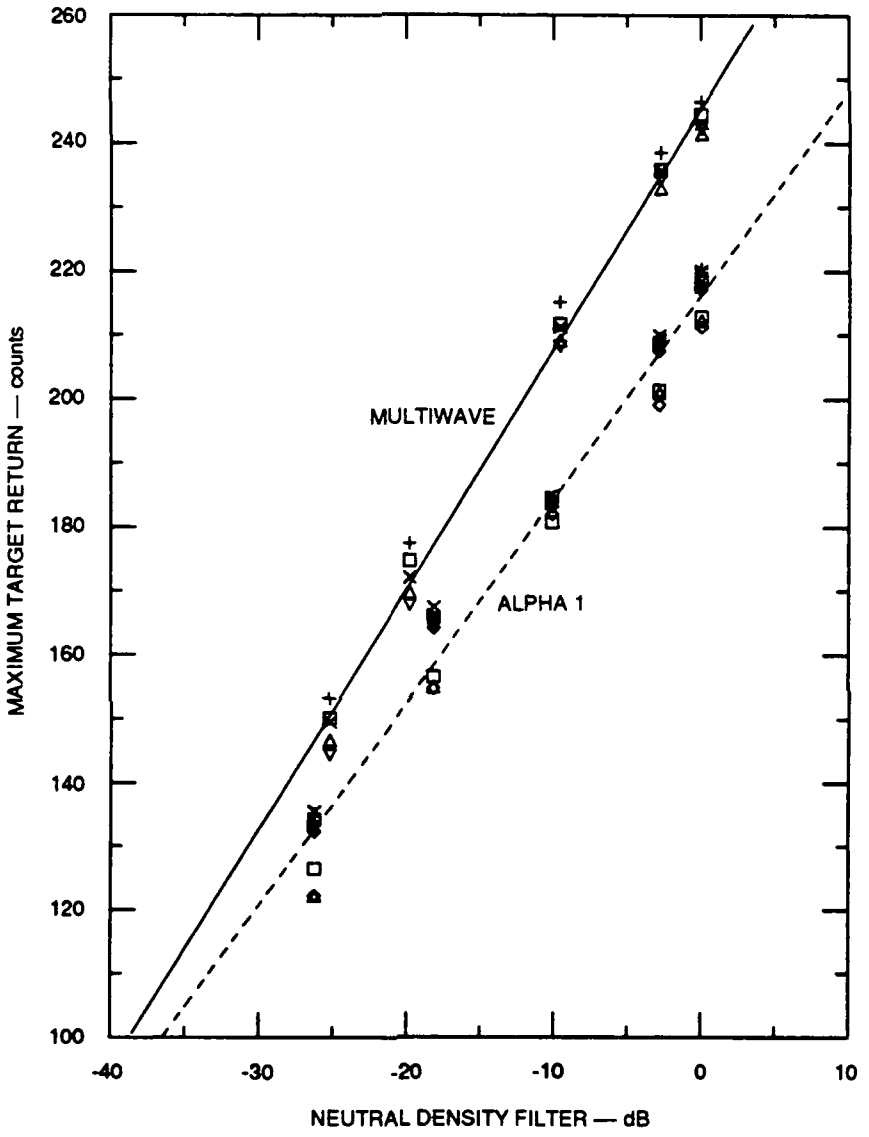

Figure 3-3. SRI lidar calibration results obtained during CECATS. Different symbols represent measurements obtained during different calibration runs; the lines represent linear least squares fits to the composite data sets for the ALPHA 1 lidar (dashed line) and the multiwavelength lidar (solid line).

Table 3-1

LIDAR CALIBRATION RESULTS

ALPHA 1 Lidar

Date	Trial	Least-squares slope [cts/dB] Value	Uncertainty	Correlation coefficient
9 May	310	3.110	0.173	0.995
10 May	022	3.157	0.131	0.997
12 May	012	3.206	0.098	0.999
17 May	212	3.288	0.170	0.996
17 May	230	3.346	0.156	0.997
17 May	441	3.166	0.156	0.996
17 May	031	3.121	0.157	0.996
18 May	130A	3.138	0.137	0.997
18 May	134B	3.141	0.138	0.997

Multiwavelength Lidar

Date	Trial	Least-squares slope [cts/dB] Value	Uncertainty	Correlation coefficient
9 May	310	3.732	0.088	0.999
12 May	012	3.680	0.110	0.999
17 May	230	3.706	0.098	0.999
18 May	130A	3.760	0.086	0.999
18 May	134B	3.911	0.075	0.999

4. DATA ANALYSIS

Three separate methods have been investigated to derive range-dependent smoke extinction coefficients from the CECATS lidar measurements. Each of these is discussed in this section.

Typically, in order to derive range-dependent atmospheric extinction coefficients from single-ended lidar returns, it is necessary to assume a relationship between the volumetric backscatter and extinction coefficients. However, if the total transmittance along the laser propagation path is known, or can otherwise be calculated, as is possible when the path is terminated by a diffusely reflecting target, then a range-dependent extinction profile can be calculated directly from the single-scattering lidar equation. However, this calculation is valid only if it can be assumed that the extinction-to-backscatter ratio is constant over the propagation path and, obviously, only if multiple scattering is negligible. This methodology was designated the target method by Uthe and Livingston [1986]. Results from its application to CECATS smoke measurements are discussed in Subsection 4.1.

An experimental technique that derives extinction profiles by utilizing nonlinear least squares methodology to define a functional relationship between the target-derived optical depth and the path-integrated lidar signal returns is discussed briefly in Subsection 4.2. This method was also discussed in detail by Uthe and Livingston [1986].

Recently, it has been shown [Kunz, 1987; Hughes and Paulson, 1988] that if measurements are available from two separate lidars located at opposite ends of a common propagation path, range-dependent extinction coefficients can be calculated analytically without the necessity for any knowledge of or assumption regarding the extinction-to-backscatter ratio. Results from attempts to apply this inversion procedure to CECATS data are presented in Subsection 4.3.

4.1 TARGET METHOD

Target returns measured by a lidar can be interpreted in terms of transmission, $T_{path}(t)$, across the lidar-to-target path according to

$$T_{path}(t) = \left[\frac{P_{rg}(t)}{P_{rg}(t_{clear})}\right]^{0.5}, \tag{4.1}$$

where $P_{rg}(t)$ and $P_{rg}(t_{clear})$ are the power backscattered from the target and measured by the detector at times t and t_{clear}, respectively, where t_{clear} represents a time of clear air atmospheric conditions (i.e., transmission = 1) along the propagation path. Figure 4-1 presents the transmission time histories derived in this manner from the target returns observed by each lidar during CECATS trial 134b. A scatterplot of the corresponding optical depths, u(t), where $u(t) = -\ln [T_{path}(t)]$, is shown in Figure 4-2. This plot

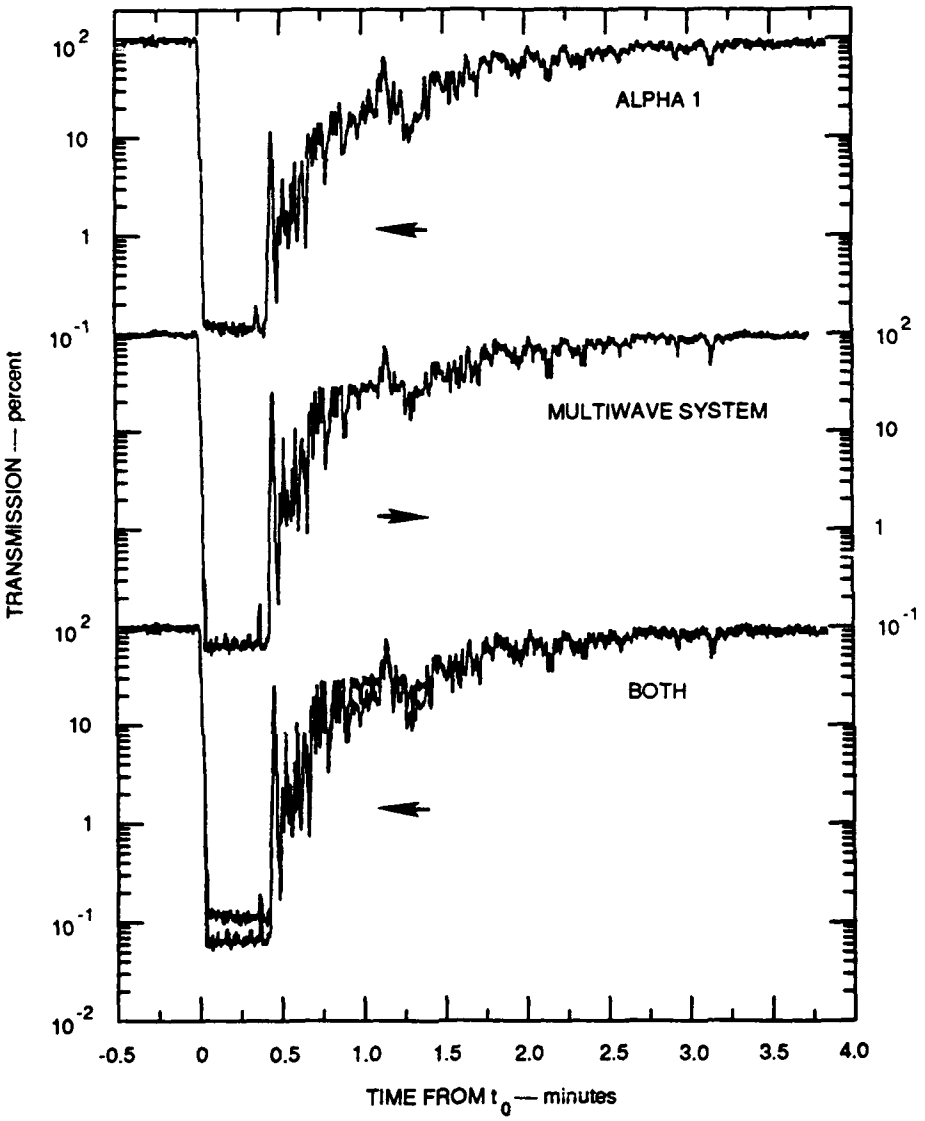

Figure 4-1. Time histories of lidar-path transmissions derived from target backscatter measurements obtained during trial 134b. Results are shown separately for each lidar in the top two traces and are superimposed in the bottom trace.

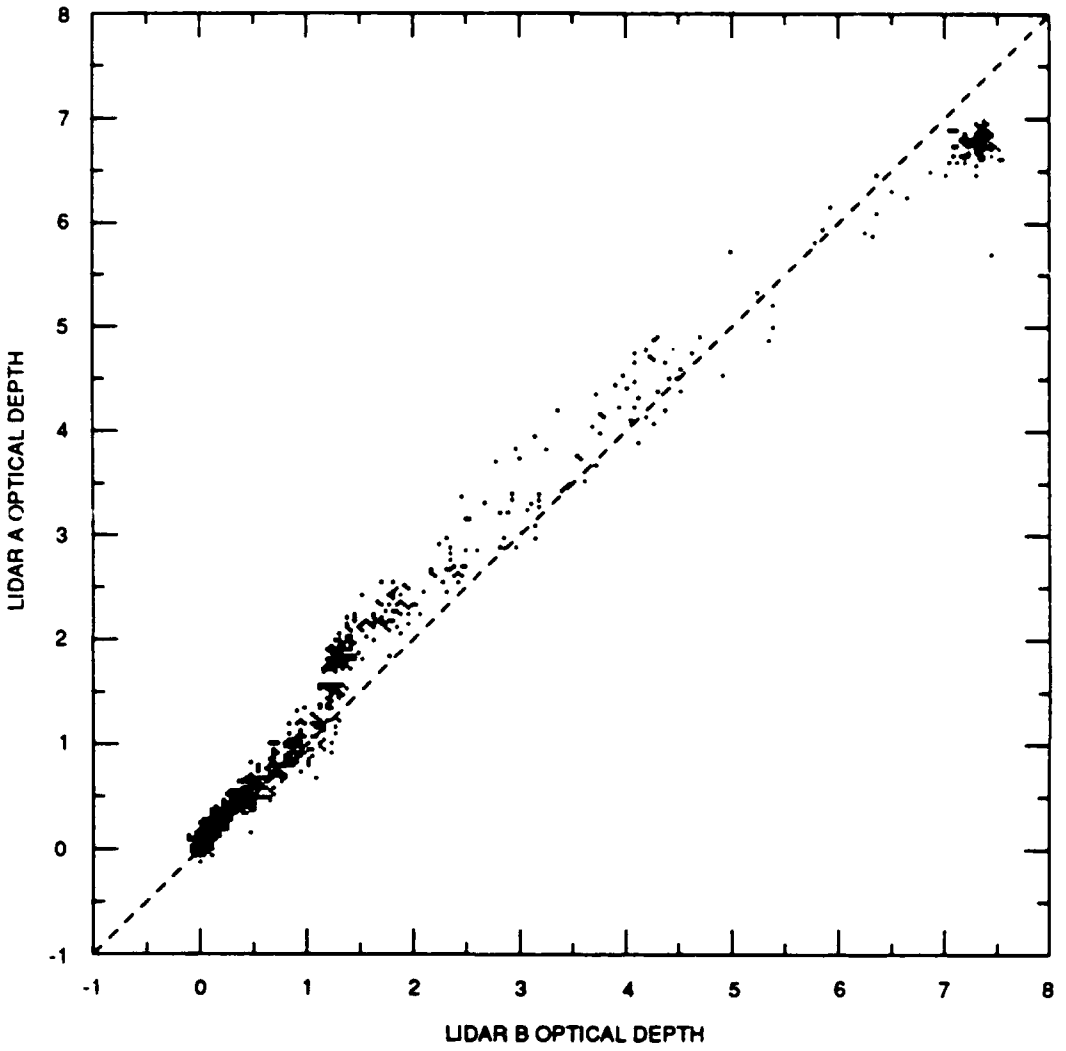

Figure 4-2. Comparison of total path optical depths derived from target backscatter measurements obtained by the two SRI lidars during trial 134b. Lidar A is the ALPHA 1 system, and Lidar B is the multiwavelength system.

was produced by pairing the data from the two lidar systems according to their proximity in time, since the two lidars did not fire at precisely the same time. The data could have been analyzed in an analogous manner by interpolating one set of lidar data to the times of the other lidar measurements. However, because the maximum time separation between lidar shots paired according to their times of transmission was less than 0.1 s, the pairing method was employed. In general, the measurements shown agree well, although for optical depths exceeding 1.2 (transmissions > 30%), the data appear well correlated but offset from the expected line of equal optical depth values. This offset may be due to a combination of the following factors: incorrect characterization of either or both of the logarithmic amplifier response curves (i.e., nonlinearity of the response curves); target irregularities; differences in the optical properties of the air volumes sampled by the two laser beams due to spatial differences in the distribution of aerosols along the propagation paths (which may be related to the small temporal differences between laser firings); or errors in the clear air (i.e., 100% transmission) target returns.

It has been shown [Fernald et al., 1972] that if the ratio of the extinction coefficient to the backscatter coefficient, $k = \sigma(r)/\beta(r)$, is constant over the range interval Δr being investigated, then the two-way transmittance $T^2(R,t)$ can be calculated from the single-scattering lidar equation as

$$T^2(R,t) = 1 - \frac{2k}{C}\int_0^R \eta(r)dr, \tag{4.2}$$

where $\eta(r)$ is the signal whose amplitude is proportional to the power received from a scattering volume at range r and is corrected for the geometric range-squared effect and transmitted energy variations, and C is a lidar system constant. Theoretically, at any time, t, the calculated total path transmittance, $T_{path}(t)$, can be used to determine the value k/C, which can then be combined with the integral of the received backscatter signals to intermediate ranges to yield a horizontal transmission profile. Since transmission is directly related to optical depth, and optical depth is just the integral of the extinction coefficient over range, the calculation of a transmission profile implies a corresponding extinction profile

$$\sigma(r,t) = \frac{du(r,t)}{dr}. \tag{4.3}$$

Previously, Uthe and Livingston [1986] used this technique, which they designated the target method because it requires use of a target to determine the value k/C, to derive extinction profiles from multiwavelength lidar measurements taken through smoke during the Smoke Week VI experiments.

They showed that the magnitude of k/C was not necessarily constant for a given type of obscurant, but rather it exhibited both gradual and rapidly fluctuating variability that, they suggested, may have been caused by pulse-to-pulse changes in lidar system performance and/or changes in the optical properties of the scattering obscurant. Hence, they concluded that, in order to utilize the target method for deriving extinction, k/C must be evaluated independently for each lidar observation. Clearly, this is a necessity if no measure of the pulse-to-pulse variation in transmitted energy is available for postmeasurement lidar signal processing, as is the case for our measurements obtained during the CECATS test. It should be noted that although we generally normalize our data to mean clear air signatures, the values of k/C still exhibit large shot-to-shot fluctuations.

The target method has been applied to the measurements obtained during trial 134b. Figure 4-3 presents contours of the calculated extinction coefficients as a function of range (from the ALPHA 1 lidar) and time from t_o for this test. In order to facilitate our comparative analyses of results from two lidar systems that did not fire at precisely the same time, we have arbitrarily defined t_o as the time corresponding to the beginning of the large transmission decrease measured by each lidar. This time will differ slightly from the official start time of the smoke release. Figure 4-3a shows the results derived from lidar A (ALPHA 1) measurements, and 4-3b shows the corresponding results from lidar B (multiwavelength lidar) measurements. Contours are shown for extinction values of 5, 10, 20, 50, and 100 km^{-1}. At these thresholds, measurements by the two lidars appear to yield similar extinction patterns and magnitudes within the smoke at times after t_o + 0.5 minutes. However, at times between t_o and t_o + 0.5 minutes, when total path transmissions measured by each lidar were about 0.1% (see Figure 4-1), the data for each lidar yield reduced extinction values on the far side (relative to the particular laser) of the smoke return.

This reduction in extinction on the far side of the smoke is shown clearly in Figure 4-4, which superimposes the range-corrected lidar signals measured by each lidar for a single shot at time t_o + 0.24 minutes. Figure 4-5 presents time histories for the two extinction data sets calculated for a 10.5-m mean range interval centered at a range of 993 m (from lidar A) for the period between t_o and t_o + 3 minutes. At this range, as a result of excessive attenuation of the laser beam through the smoke, lidar B grossly underestimates the amount of extinction, as is evident in Figure 4-4. Figure 4-6a presents a scatter plot for the extinction coefficients derived from measurements obtained by the two lidars between times t_o and t_o + 3 minutes. There are a significant number of lidar A extinction points that exceed those of lidar B. These outliers result from the reduction in lidar B-derived extinction on the far side of the smoke at times between t_o and t_o + 0.5 minutes, as is evident by their absence in Figure 4-6b, which shows the analogous plot for the period after t_o + 0.5 minutes. Similar comparisons between the extinction coefficients calculated from the two sets of lidar measurements at other ranges are not shown, but verify this behavior.

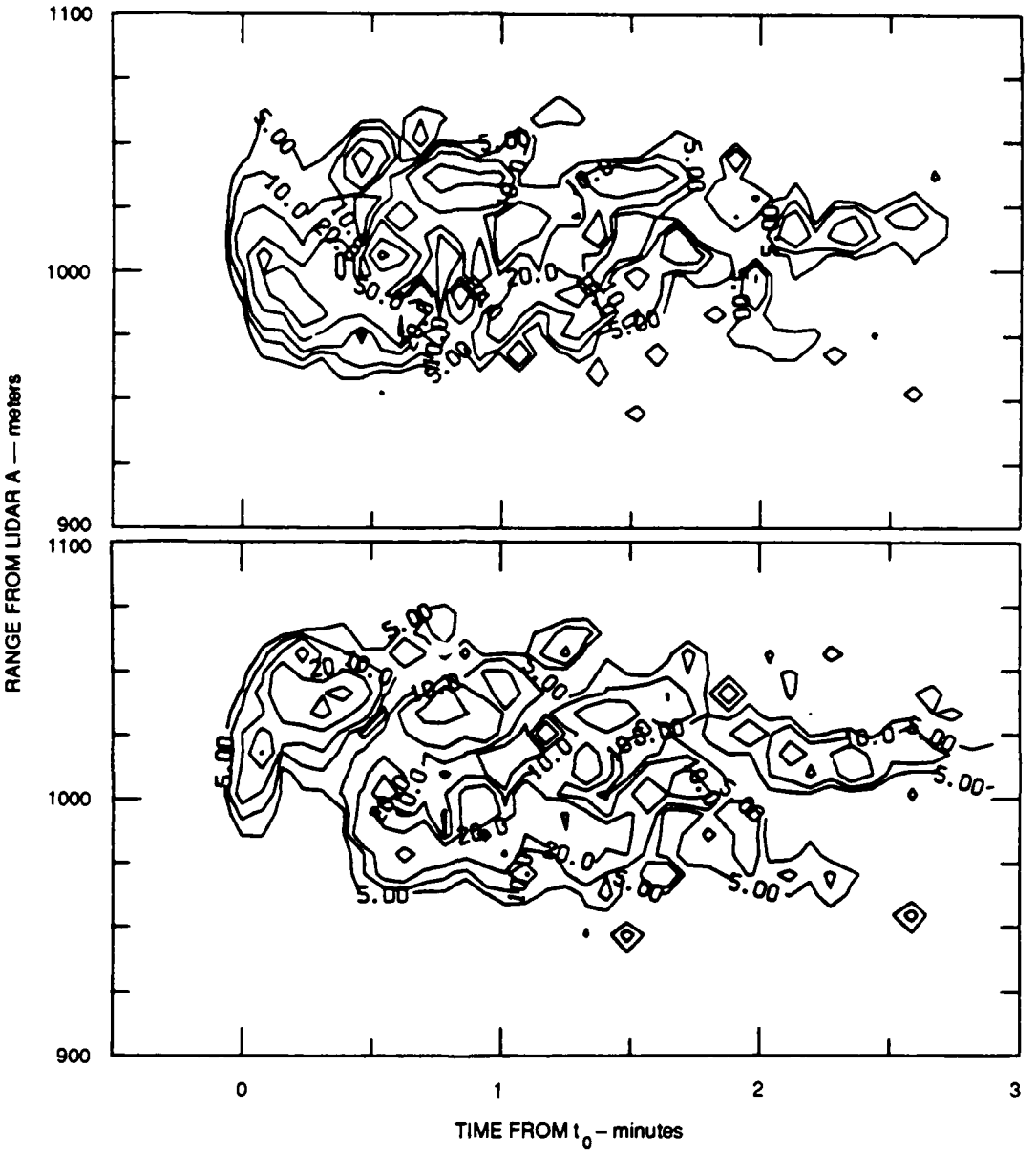

Figure 4-3. Contours of target-derived extinction values [km^{-1}] as a function of range (from ALPHA 1) and time for trial 134b for (a) the ALPHA 1 system and (b) the multiwavelength system. Contours represent averages over ten shots and five range bins (7.5 m).

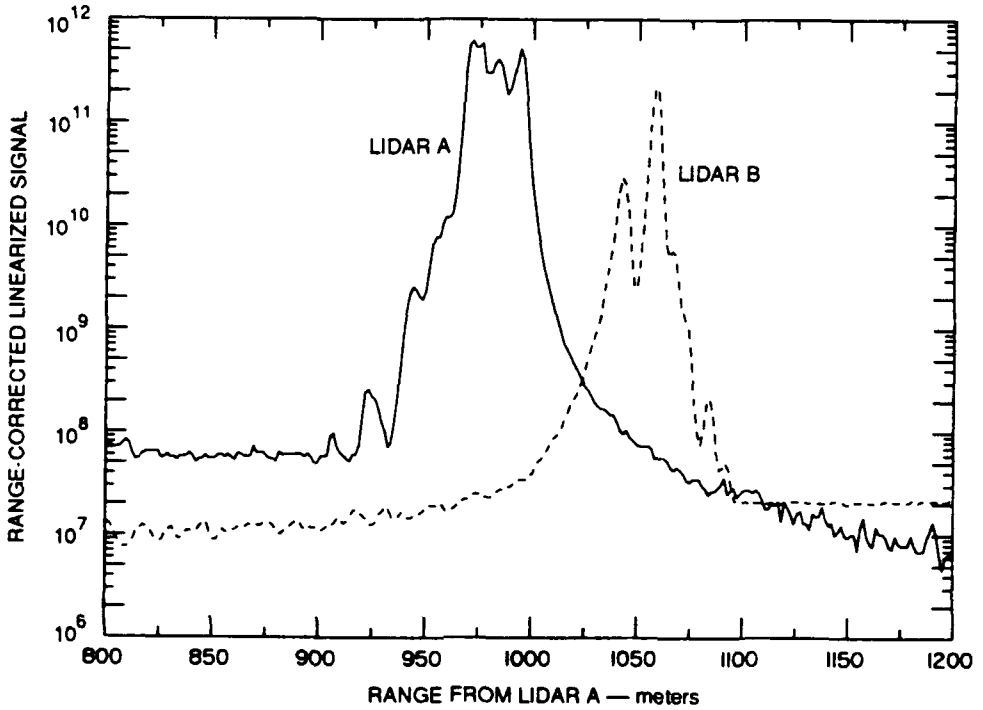

Figure 4-4. Range-corrected backscatter measurements obtained during trial 134b at time = t_0 + 0.24 minutes.

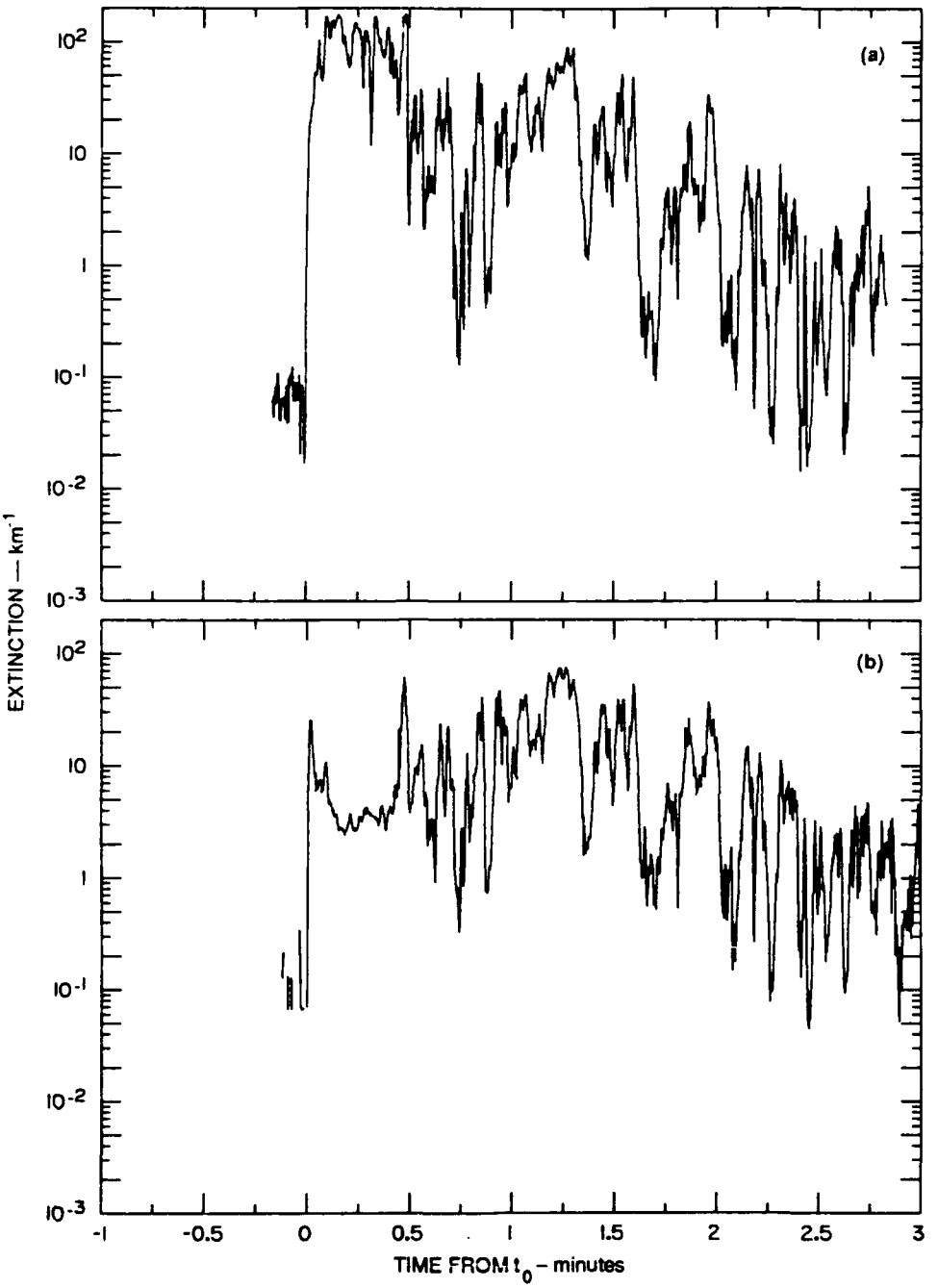

Figure 4-5. Time histories of target-derived extinction coefficients calculated for a 10.5-m mean range interval centered at a range of 993 m (from Lidar A) for the period between t_0 and t_0 + 3.0 minutes (trial 134b): (a) Lidar A, and (b) Lidar B.

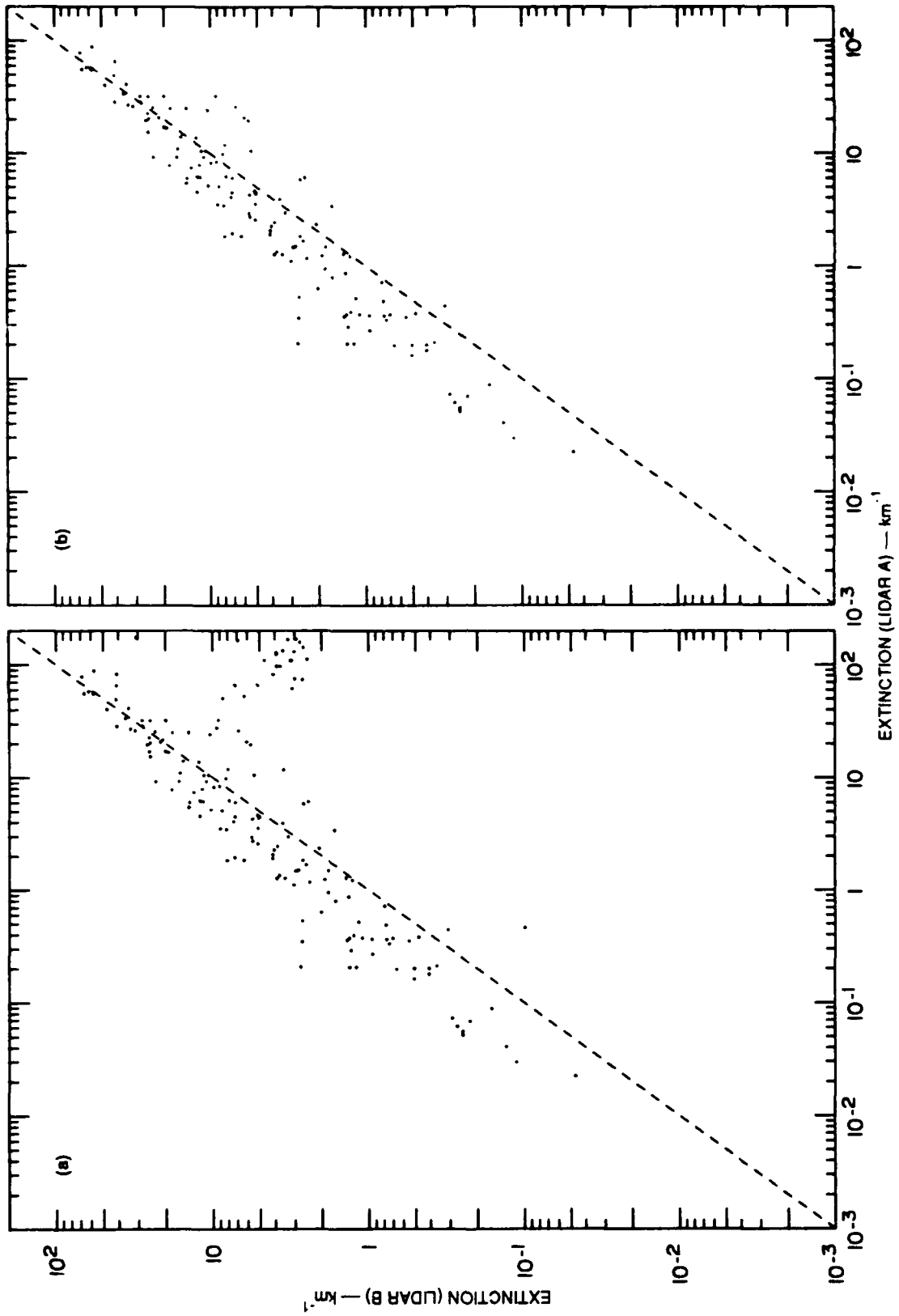

Figure 4-6. Comparison of the target-derived extinction values at a mean range of 993 m, as shown in Figure 4-5, for the periods (a) t_0 to t_0 + 3.0 minutes and (b) t_0 + 0.5 to t_0 + 3.0 minutes.

Figure 4-7 presents the relative backscatter signatures observed by each lidar at times 1.0, 1.5, and 2.0 minutes after t_o, after software removal of the range-squared dependence and application of the logarithmic amplifier linearization function. No normalization to transmitted energy or to clear-air profiles has been performed. The total path transmissions measured at these times were 23%, 30%, 56% for lidar A, and 17%, 30%, 56% for lidar B. Each lidar signature exhibits the expected behavior for measurements taken through a relatively dense obscurant--that is, a series of sharp maxima and minima superimposed on a generally decreasing signal with increasing distance (penetration) through the attenuating cloud. However, the most important point to note in these graphs is that both lidars observed relative backscatter maxima and minima at the same or nearly the same locations within the smoke. This result is observed in all the CECATS data that have been analyzed.

The calculated extinction coefficients corresponding to the data shown in Figure 4-7 are presented in Figure 4-8. In clear air at ranges on the far side of the smoke, the extinction values derived using the target method exceed those calculated on the near side of the plume for each lidar. The magnitude of these differences is greater for greater smoke optical depths (smaller path transmittance), as is evident in comparing the results shown in Figures 4-8a or 4-8b with those shown in 4-8c. These values occur because clear-air atmospheric backscatter returns on the far side of the smoke are below the minimum threshold of detection of each lidar system, because of attenuation of the laser beam through the smoke. Because the measured signals at these ranges are noise limited, application of an attenuation correction to these data using the target method yields extinction values that are too high and, clearly, not valid.

4.2 EXPERIMENTAL DATA METHOD

Previously, Uthe (1981) and Uthe and Livingston (1986) derived relationships between target-derived optical depths and path-integrated lidar signals for smoke and dust obscurants. In particular, Uthe and Livingston (1986) used a nonlinear least squares fitting technique to derive the parameters a_1 and a_1 in the expression

$$u(\psi) = a_1\psi[1 - \exp(-a_2\psi)], \tag{4.4}$$

where u is the optical depth evaluated from the target return method and ψ is the path-integrated lidar signal. They then calculated extinction profiles for individual shots by evaluating this expression directly for lidar signals integrated to intermediate ranges. In comparing extinction coefficients derived from this expression with corresponding values derived using the target method and the Klett [1981] method, they concluded that the experimental method might be more appropriate for deriving extinction

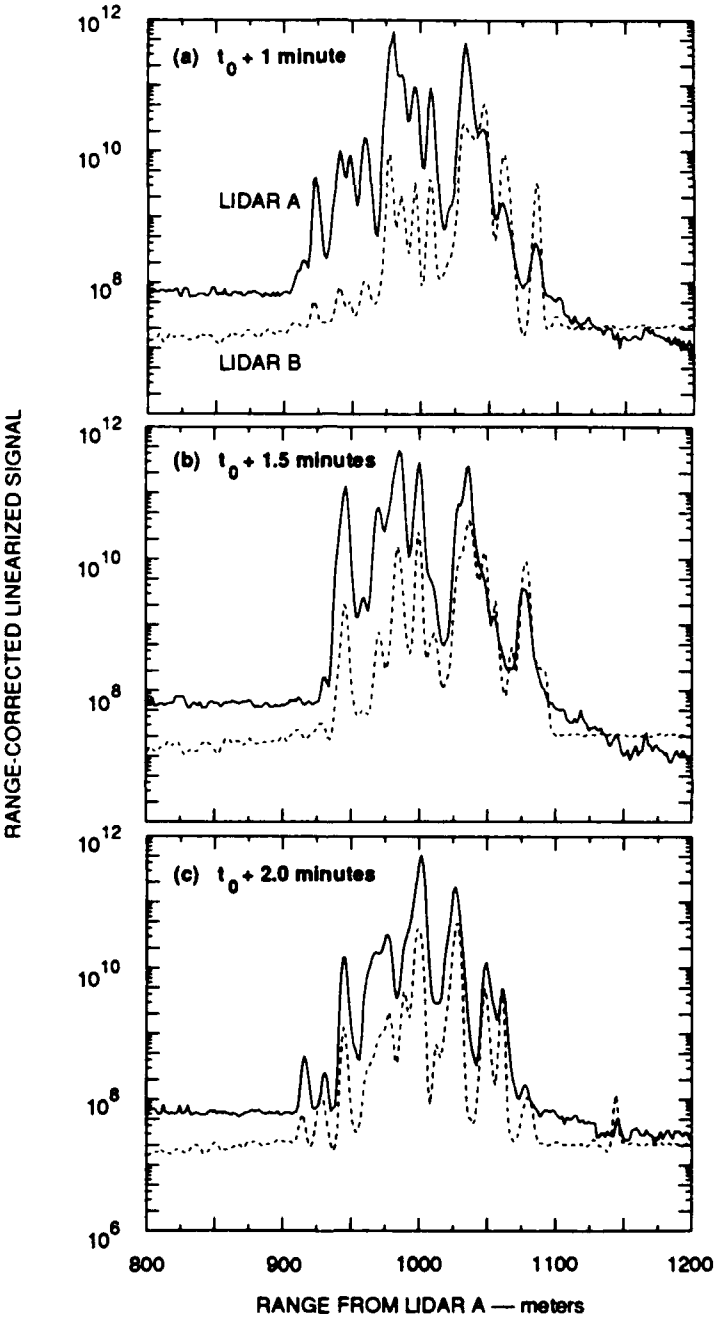

Figure 4-7. Relative backscatter signatures (after adjustment for inverse range-squared dependence and application of linearization function) measured by the two lidars during trial 134b at times (a) 1.0, (b) 1.5, and (c) 2.0 minutes after t_0.

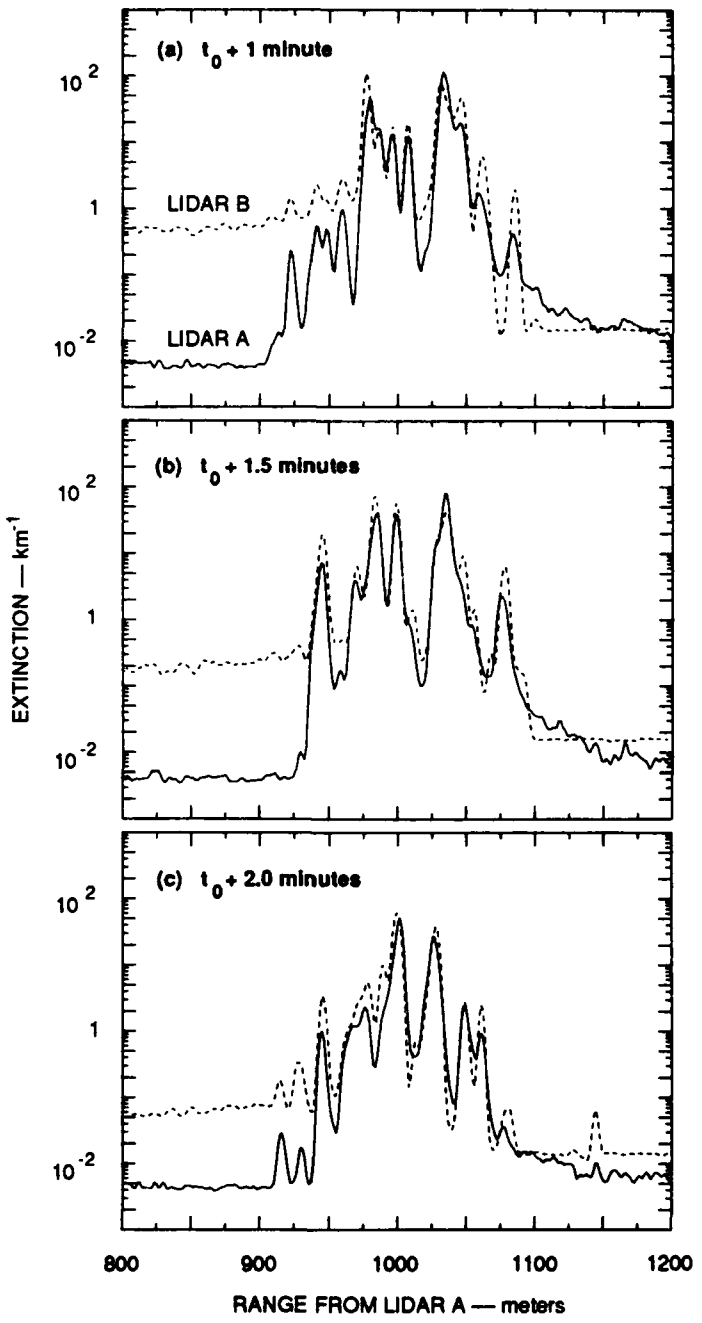

Figure 4-8. Target-derived, range-dependent extinction coefficients corresponding to the backscatter measurements shown in Figure 4-7.

profiles through relatively dense smokes because it includes multiple-scattering effects, whereas each of the other methods is based on the single-scattering lidar equation.

We have evaluated this analysis technique for smoke measurements taken by each lidar during trial 134b. Plots of optical depth versus path-integrated lidar signal are shown in Figure 4-9 for the ALPHA 1 and multiwavelength lidar systems. The dashed lines represent the nonlinear least squares fits (and associated uncertainty estimates) of Equation (4.4) to the measured data. Clearly, the expression given is a poor descriptor of the actual data measured by the ALPHA 1 lidar for optical depths that exceed 1.5 or 2. For data obtained by the multiwavelength lidar, the expression appears inappropriate over the entire range of optical depths. In fact, it is apparent from these data that no unique relationship exists between optical depth and path-integrated lidar signal for optical depths exceeding 2 for the ALPHA 1 lidar and 1 for the multiwavelength system. In light of these results, we did not pursue this inversion technique further.

4.3 ANALYTICAL TWO-LIDAR INVERSION METHOD

The two-lidar inversion technique is an analytical method for inverting measurements taken by two separate lidars located at opposite ends of a common propagation path. Following Hughes and Paulson (1988), we consider the case of two lidars separated by a distance d. If the origin of the propagation path is assigned to the lidar 1 location, then the single-scattering lidar equation determines the logarithmic, range-compensated power S(r) received by lidar 1 from a scattering volume at range r as

$$S(r)_1 = \ln K_1 + \ln[\beta(r)] - 2\int_0^r \sigma(r')dr', \tag{4.5}$$

and that received by lidar 2 as

$$S(r)_2 = \ln K_2 + \ln[\beta(r)] - 2\int_r^d \sigma(r')dr', \tag{4.6}$$

where the K_i are lidar system constants, and $\sigma(r)$ and $\beta(r)$ are the volume extinction and backscatter coefficients, respectively. If Mie single-scattering theory is assumed to apply, then subtraction of the above equations followed by subsequent algebraic manipulation of the limits of integration yields the

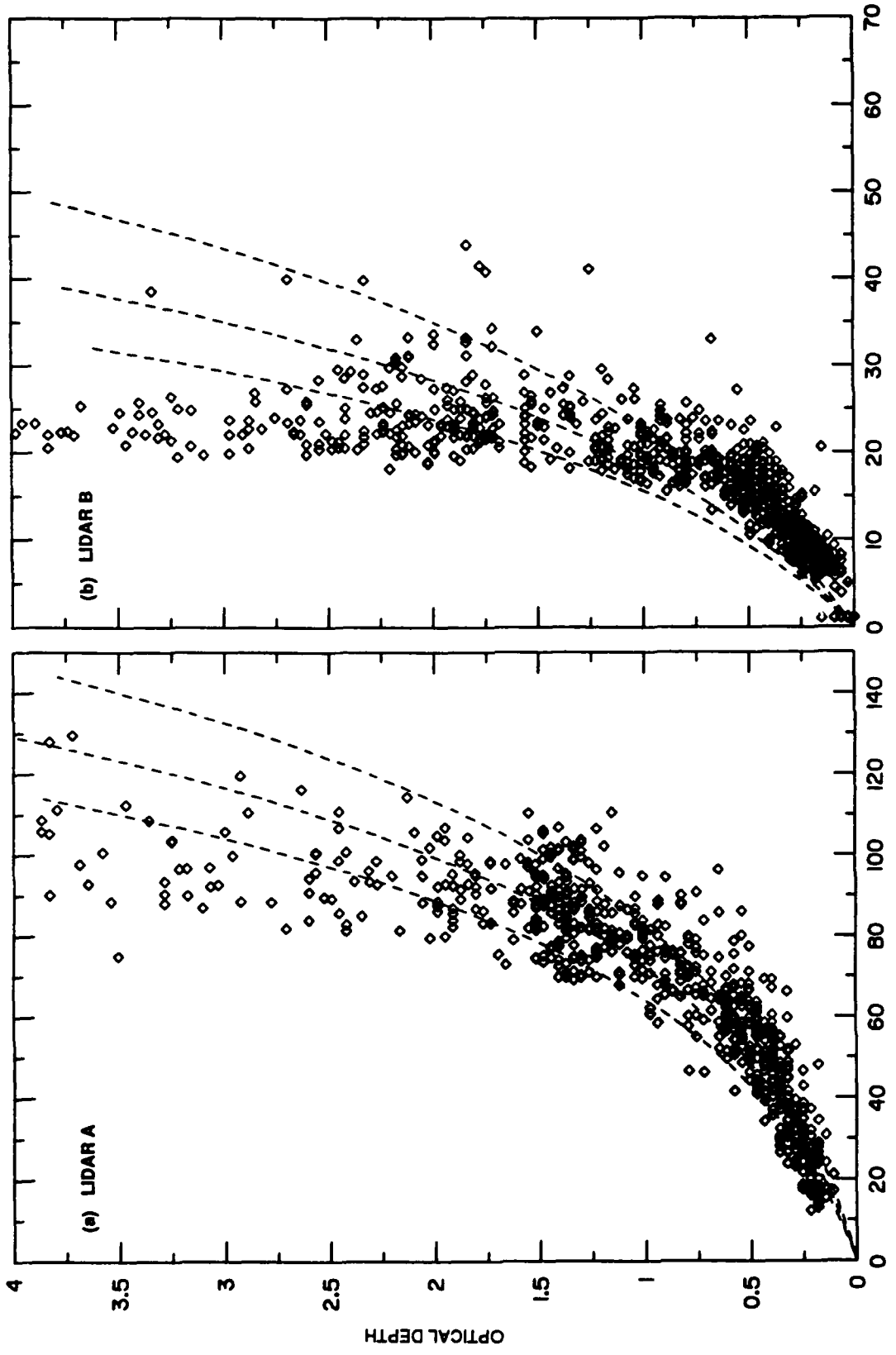

Figure 4-9. Optical depth as a function of path-integrated relative backscatter signals for the (a) ALPHA 1, and (b) multiwavelength lidar systems.

following expression for the difference:

$$S(r)_1 - S(r)_2 = \ln(K_1/K_2) - 4\int_0^r \sigma(r')dr' + 2\int_0^d \sigma(r')dr'. \quad (4.7)$$

The range-dependent extinction profile $\sigma(r)$ follows directly from Equation (4.7)--namely,

$$\sigma(r) = -\frac{1}{4}\frac{d}{dr}[S(r)_1 - S(r)_2]. \quad (4.8)$$

Hughes and Paulson (1988) used this technique successfully to calculate range-dependent extinction coefficients from a limited number of measurements taken along a 1-km path near San Diego, CA, during a period of reduced visibility and spatially and temporally varying atmospheric conditions. The maximum calculated extinction coefficient for the two cases that they reported was 3 km^{-1}, and the optical depths were 0.76 and 1.06.

We have been unsuccessful in utilizing this technique to invert the lidar measurements we obtained during CECATS. In order to demonstrate the problems we encountered, in this section we apply this method to measurements taken through clear air before trial 134b and through smoke during the trial at times when the calculated total path transmittances exceeded 60% (corresponding to an optical depth of 0.5). As shown in Figure 4-1, path transmittances near 0.1% (optical depths ≥ 7) were observed during this trial. First, we shall examine the clear-air measurements.

Figure 4-10a presents the logarithmic, range-corrected signals, S(r), for single-shot measurements taken through clear air by each lidar prior to the smoke release of trial 134b. Each trace has been normalized to a longer-period mean clear-air trace to minimize laser energy and other lidar system-dependent variabilities. Figure 4-10b shows the signal differences, $S(r)_1 - S(r)_2$, calculated directly from the signatures shown in Figure 4-10a, and also calculated by taking 21-point (31.5-m) running averages of these data. The resultant horizontal extinction coefficient profile is presented in Figure 4-10c, where the values have been calculated from Equation (4.8) using a 3-point central differencing scheme applied to the 21-point running average difference curve. Clearly, the variability in the resultant extinction profile is unacceptably large, due, in part, to the differentiation scheme. In an effort to further reduce this variability, 21-point running averages of the derivatives have also been calculated; these are also shown in Figure 4-10c. This is equivalent to taking the derivative of the difference curve with a running range interval of 21 points. Regardless of the derivative scheme employed, however, the resultant extinction curve exhibits oscillations of 1 to 2 km^{-1} about a near-zero mean extinction value, resulting in nonphysical (negative) values over several ranges.

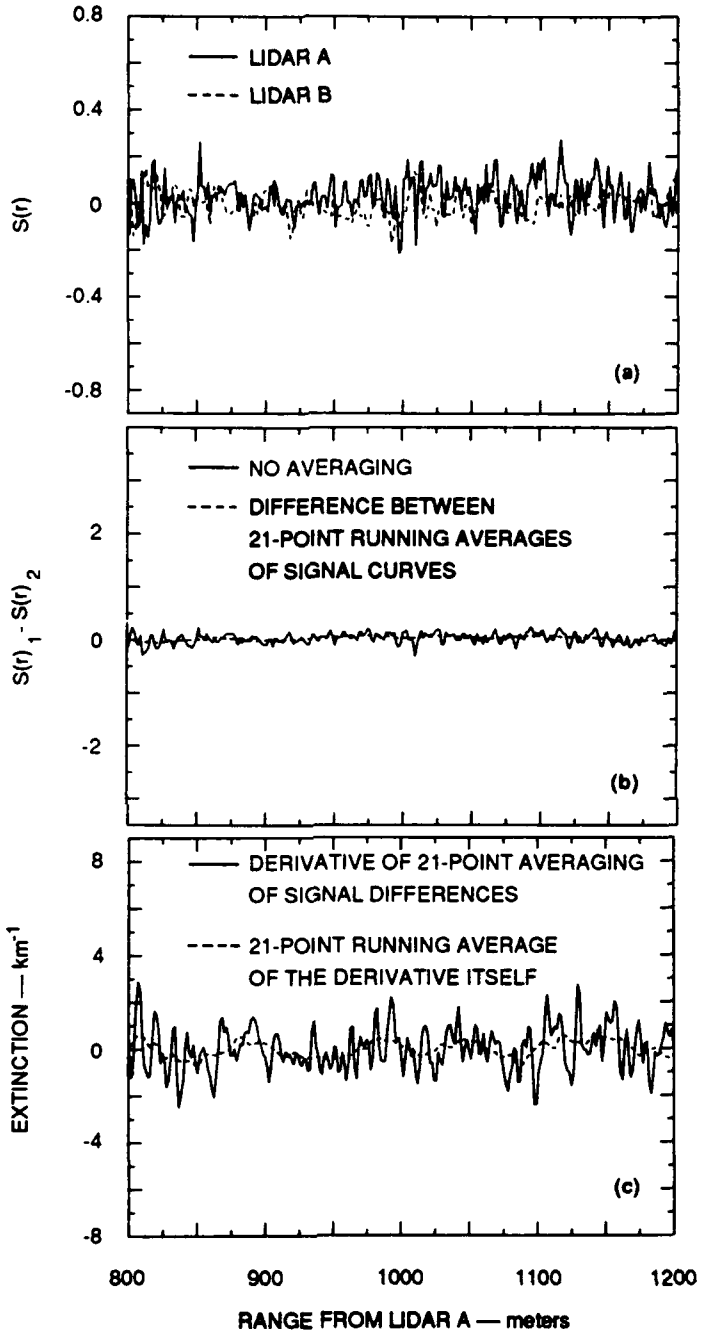

Figure 4-10. Application of analytical two-lidar inversion technique to clear-air backscatter measurements obtained prior to trial 134b: (a) logarithmic, range-corrected signals, S(r); (b) signal differences; (c) model and retrieved horizontal extinction profile.

Hence, the sensitivity of this inversion technique when applied to clear-air measurements taken with our lidar systems appears to be on the order of 1 to 2 km^{-1}. In other words, these results imply that the noise components in our measured backscatter signals, at least through scattering volumes with very small optical depths (that is, clear air), are too large to allow successful inversion using the analytical two-lidar technique. Certainly, this is disappointing, as Hughes and Paulson [1988] were able to derive extinction coefficients of magnitude 0 to 3 km^{-1} using this method. However, in order to do so they were forced to utilize an 11-point (82.5 m) running average to calculate the S(r) curves and a 15-point (112.5 m) running range interval to calculate the derivatives. Unfortunately, application of running average widths or derivative range intervals of this magnitude does not significantly improve our clear-air results. Next, we shall examine the results of applying this inversion technique to smoke measurements, to determine if the data are more amenable to inversion when the optical depths are higher.

Figure 4-11 presents analogous plots for lidar measurements made during trial 134b at a time when the target-derived transmissions were 66% for Lidar A and 69% for Lidar B (optical depths of about 0.4). The signal differences are shown both for no averaging and for the case where the difference curve was calculated from 41-point (61.5 m) running averages of the signal curves. It may be recalled from Equation (4.8) that the extinction coefficient is proportional to the negative of the slope of the signal difference curve. Clearly, the difference curve presented in this figure is bound to yield negative extinction values for ranges between 875 and 990 m, where the slope is positive. This is confirmed in the corresponding extinction profile shown in Figure 4-11c. For ranges greater than 990 m, where the mean slope is negative, the extinction values calculated using a derivative function with a 21-point running range interval are positive and realistic. However, the magnitudes are clearly very sensitive to the range interval spacing or the averaging interval of the derivative.

Results for two additional times, corresponding to transmissions of about 83% and 91%, are presented in Figures 4-12 and 4-13. For each time, which represents a single lidar shot for each lidar, the signal returns have been normalized to lidar-dependent mean clear-air signatures and are shown before any averaging. The signal differences, however, represent differences between 21-point running averages of the signals. Evidently, the two lidars did observe nearly the same volume of smoke, as most signal maxima and minima appear at the same, or nearly the same, location. Unfortunately, however, it is equally evident that the large positive and negative excursions of the resultant signal difference curves are bound to yield nonphysical (negative) extinction coefficients over large regions of the signatures, regardless of what type of signal smoothing or derivative function is applied to the data.

Analyses of these and other lidar shots (which yield similar results, regardless of the optical depth magnitudes) taken through smoke particulates generated during the CECATS study force us to conclude that these data cannot be inverted to yield extinction coefficients using the two-lidar technique. In Sections 5 and 6 we examine reasons why this may be the case.

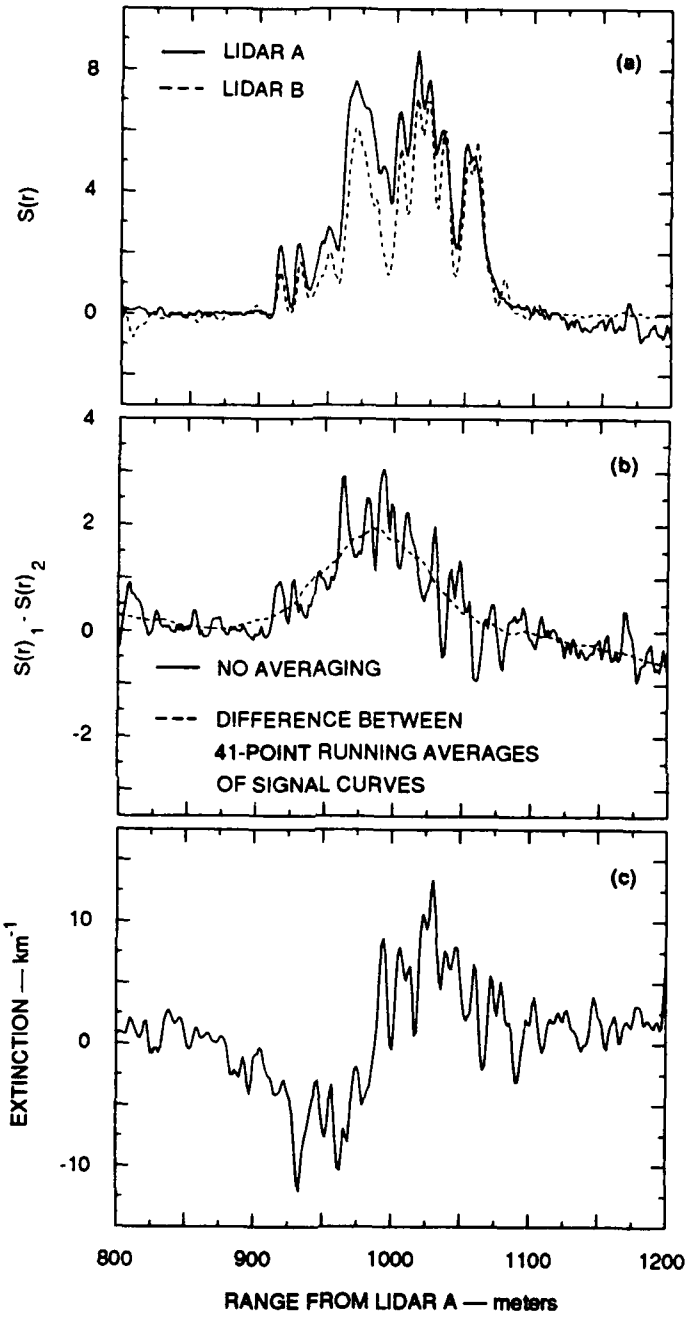

Figure 4-11. Application of analytical two-lidar inversion technique to single-shot smoke measurements obtained during trial 134b. Target-derived path transmissions were about 67% for this time. Extinction coefficients were calculated using a derivative function with a 21-point running range interval.

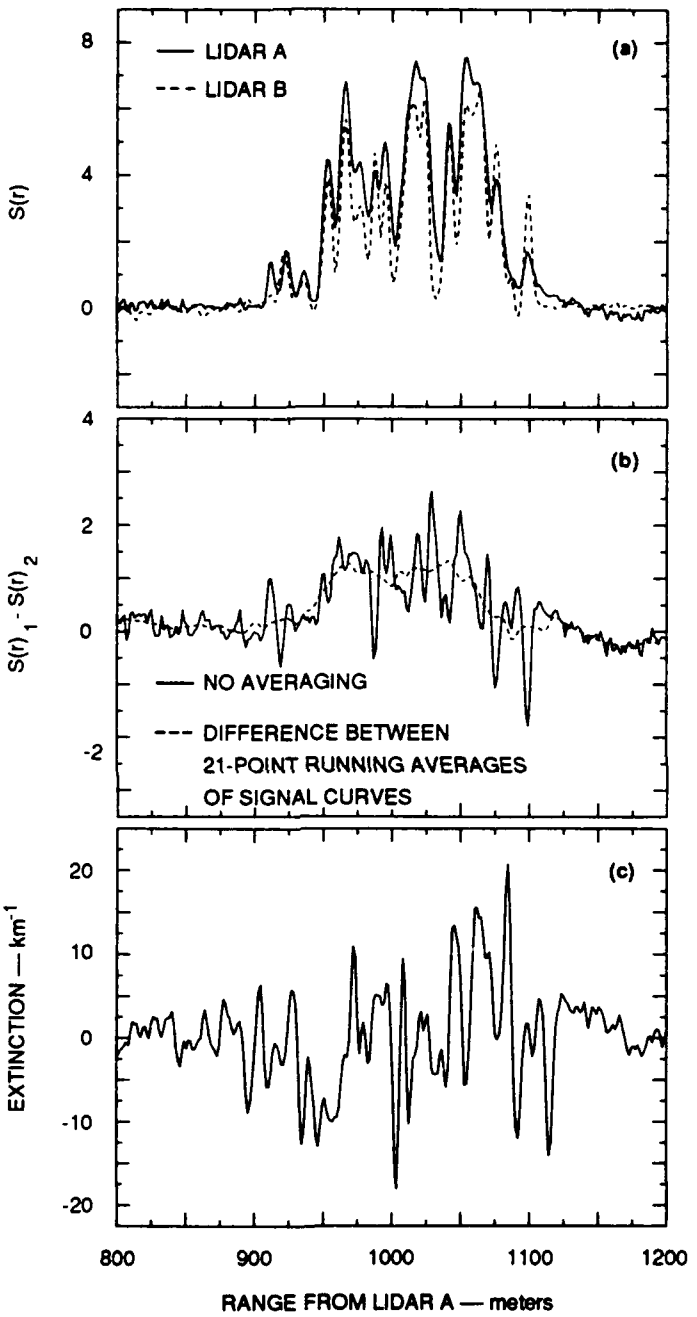

Figure 4-12. Application of analytical two-lidar inversion technique to smoke measurements obtained during trial 134b for shots with target-derived path transmissions of about 83%.

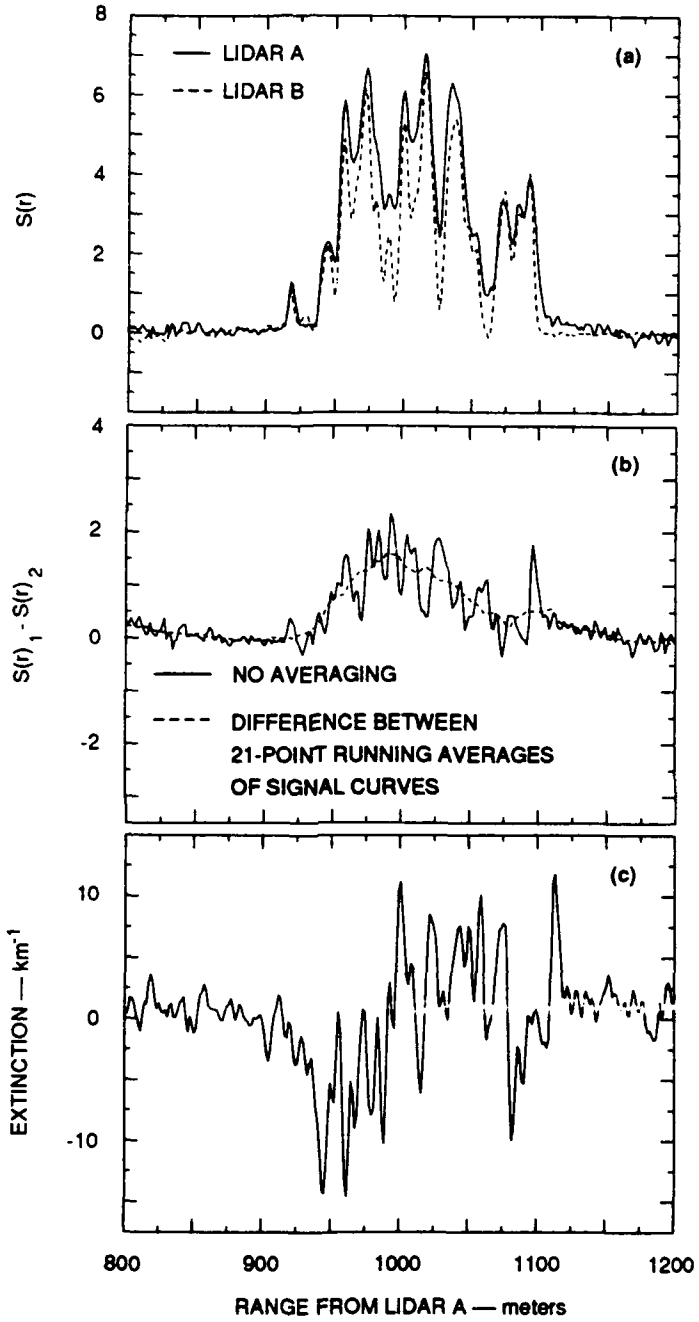

Figure 4-13. Application of analytical two-lidar inversion technique to smoke measurements obtained during trial 134b for shots with target-derived path transmissions of about 91%.

5. INVESTIGATION OF LIDAR SYSTEM RESPONSE

In this section, we investigate the response of each lidar system to signal attenuation induced by the placement of optical neutral density filters in the laser beam and also to attenuation by smoke aerosols. Since the shape of the signal dropoff after target impaction is a measure of the response of the logarithmic amplifier, we examine signals in this region. First, we look at target returns measured through clear air with and without the use of optical filters of known different optical densities in the lidar optical path. These signatures are then compared to target returns of similar magnitude obtained through smoke.

Figure 5-1 shows representative ALPHA 1 (Lidar A) backscattered signals for a single laser shot at times (i.e., ranges) before and after target impaction. Values are plotted in actual digitizer units (counts), where each order of magnitude (10 dB) of dynamic range in the logarithmic amplifier response is equivalent to about 32 counts. Three separate traces are shown. One represents the unattenuated

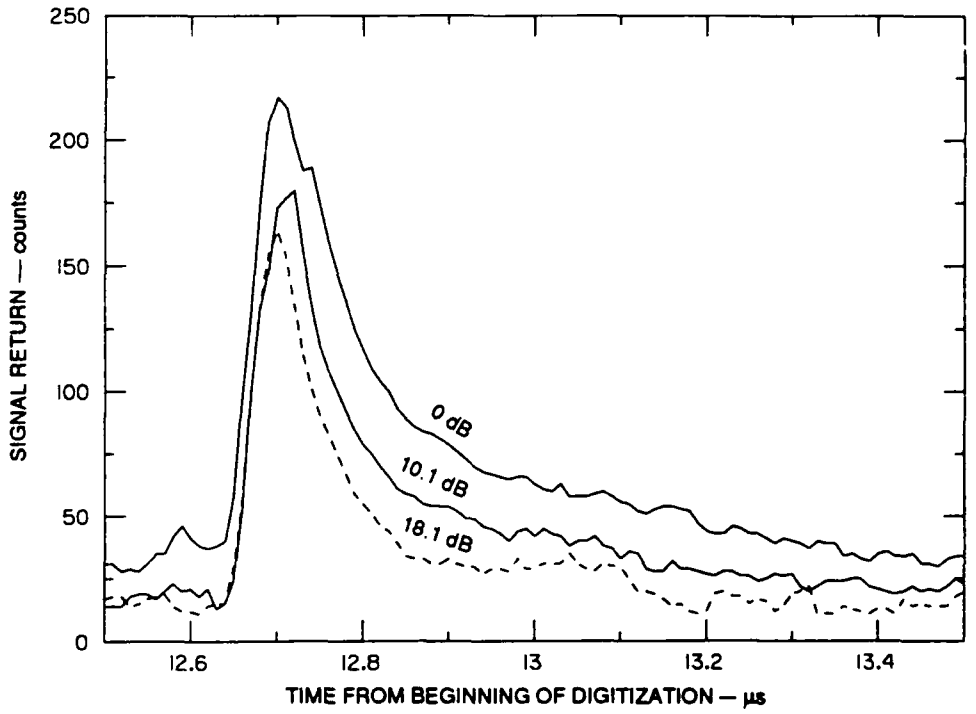

Figure 5-1. Representative ALPHA 1 lidar clear-air backscatter signatures before and after target (shown by peak) impaction. Traces are shown for one shot with no artificial attenuation, and also for shots acquired with the use of attenuating optical neutral density filters of 10.1 and 18.1 dB, respectively.

measurement through clear air, and the other two were obtained by inserting optical filters of 10.1 and 18.1 dB, respectively, in the optical path. Several points should be noted in examining this figure. First, the maximum target return decreases with increasing attenuation. This is the expected result, of course, and it forms the basis for calibration of the logarithmic amplifier, which was discussed in detail in Section 3. Second, the slope of the signal rise to target peak is much steeper and more uniform than the slope of the signal dropoff after target impaction. This can be seen by features of the unattenuated trace. Whereas the rise from pretarget background to target peak takes about 50 ns (5 digitizer sample points), the dropoff from peak to full-width half maximum (FWHM), which has a width of about 120 ns, takes about twice that long (90 to 100 ns, or 9 to 10 sample points), and then decays at a much slower nonlinear rate before finally reaching the pretarget background value after about 600 ns (60 sample points). The final, and perhaps most important, point is that both the FWHM value of the target return peak and the duration of the total decay to pretarget background decrease with increasing attenuation.

Having characterized the time response behavior of the lidar system logarithmic amplifier to optically attenuated signals backscattered through clear air from a diffusely reflecting target, we now examine whether this same type of response is observed in measurements taken through smoke obscurants. If the behavior is essentially the same, then this fact should enable us to distinguish, to a large extent, whether our lack of success in deriving smoke extinction profiles using the two-lidar technique was caused by multiple scattering by the smoke particles or by the response of the logarithmic amplifier. This is important because if the problem was introduced by the lidar hardware, corrections may be possible to make the two-lidar method a viable means for quantitative evaluation of aerosol obscurants.

In Figure 5-2, the 18-dB filter-attenuated target return trace is superimposed on a corresponding lidar signature, with a peak target return (corresponding to a path transmission of 14%) of nearly equal magnitude, that was measured through a smoke obscurant. These measurements were taken within 4 minutes of each other. The shapes of the peaks are virtually identical. Figure 5-3 overplots target returns measured through the smoke on four consecutive lidar shots (with calculated path transmissions from 2% to 14%) beginning with the shot shown in the previous Figure (5-2). These returns also exhibit a decrease in pulse width -- that is, a more rapid posttarget decay to the pretarget background signal level -- with increasing smoke extinction. The pulse shape for the smallest amplitude peak indicates that the response of the logarithmic amplifier over the first 3 to 3.5 orders of magnitude (~95 to 115 counts) is more uniform (that is, more linear) than for higher backscatter signals. If multiple scattering were significantly affecting the laser pulse propagation, one would expect the measured target return through dense smoke to be widened as a result of laser energy that is scattered back into the beam in the forward direction and, hence, is available for subsequent reflection by the target. There is

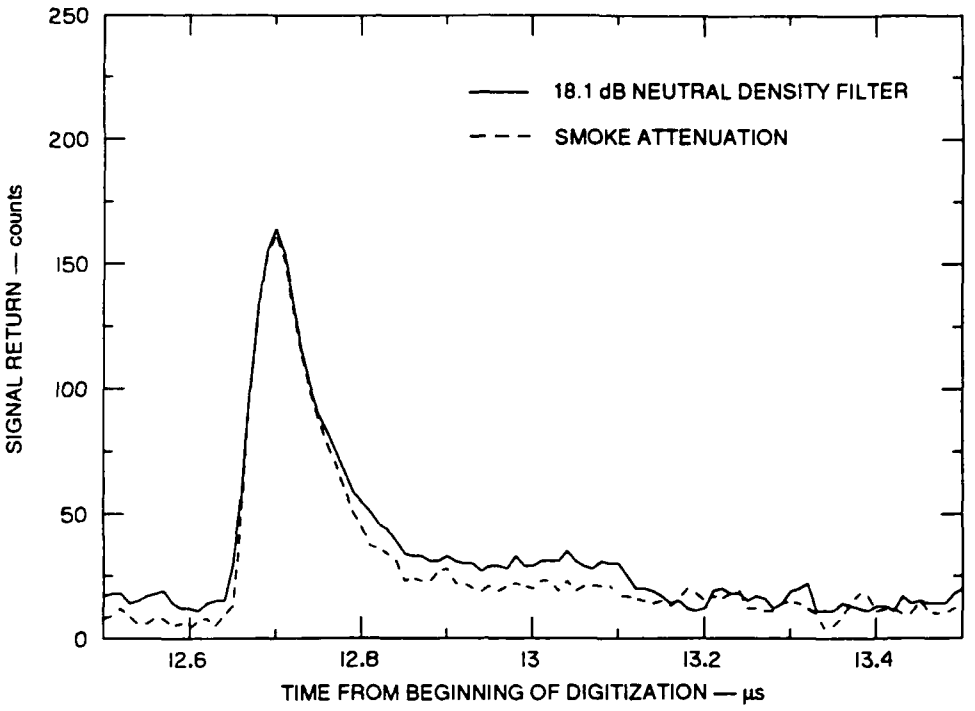

Figure 5-2. Comparison of ALPHA 1 lidar backscatter signal traces near the target for a measurement obtained through clear air with the use of an 18.1-dB neutral density filter and for a measurement taken through smoke about 4 minutes later.

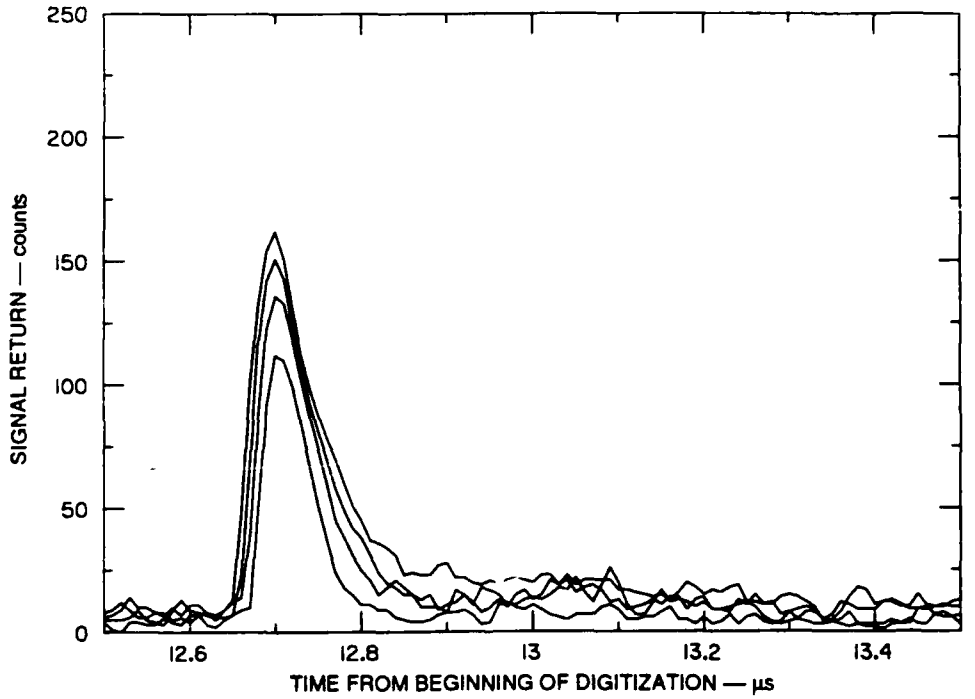

Figure 5-3. ALPHA 1 lidar backscatter target returns for four consecutive shots taken through smoke, beginning with the smoke measurement shown in Figure 5-2.

no evidence in Figure 5-2 and Figure 5-3 to indicate that this signal stretching has occurred. Examination of corresponding returns for other smoke measurements during CECATS reveals similar results.

Next, we examine the response of the multiwavelength lidar system, Lidar B. Figure 5-4 shows representative near-target backscatter returns for measurements taken with this system through clear air with and without the use of attenuating optical filters. This figure is analogous to Figure 5-1 for Lidar A. It depicts four separate backscatter signatures: one measured with no filter, and one each with filters of 9.6, 19.8, and 25.8 dB, respectively. Values are in digitizer counts, where the conversion is approximately 38 counts/10 dB. Clearly, the response characteristics of the Lidar B logarithmic amplifier are different from those of the Lidar A logarithmic amplifier. In particular, the Lidar B target returns shown in Figure 5-4 indicate a sharper, narrower response. For the unattenuated signal, the rise time is about 40 ns (four digitizer samples), followed by a sharp dropoff to FWHM (of about 50 ns width) in about 30 ns. Beyond this point, the decay rate decreases slightly to the 40% peak point, from which it slows considerably until the signal becomes oscillatory and recovers to its pretarget background level after approximately another 500 to 600 ns. The duration (width) of the slowly-decreasing ramp decreases significantly with increasing attenuation, and almost disappears completely for a 25.2-dB attenuating filter. The shape of the target peak is similar for measurements taken through smoke, as shown in Figure 5-5, which presents data traces for three consecutive shots (with calculated path transmission between 1% and 7%) taken about 3 minutes after the calibration. Again, the signal shape shows no indication of pulse stretching due to multiple scattering.

Based on the above analyses, we conclude that the logarithmic amplifier used in the ALPHA 1 (Lidar A) system yields a uniform, reproducible response to about 3 orders of magnitude, and the corresponding logarithmic amplifier used in the multiwavelength (Lidar B) system is reliable to about 3.5 to 4 orders of magnitude. Comparison of the shape of the target returns measured through smoke with those obtained using optical filters of varying optical density strongly suggests that the amount of multiply scattered light affecting the smoke measurements did not appreciably affect the transmitted beam. Hence, it alone cannot be used to explain the failure of the two-lidar inversion technique to derive range-resolved smoke extinction values. Since we have been unable to successfully apply the two-lidar method to smoke plumes of even low optical depths, we are forced to conclude that the failure of the method is attributable to use of the logarithmic amplifiers. Despite the fairly uniform decay of the logarithmic amplifiers over the first few orders of signal magnitude, it seems that the presence of even a few tens of nanoseconds delay in amplifier response, when combined with a spatially inhomogeneous smoke cloud, introduces a signal noise component that dominates the inversion over much of the propagation path.

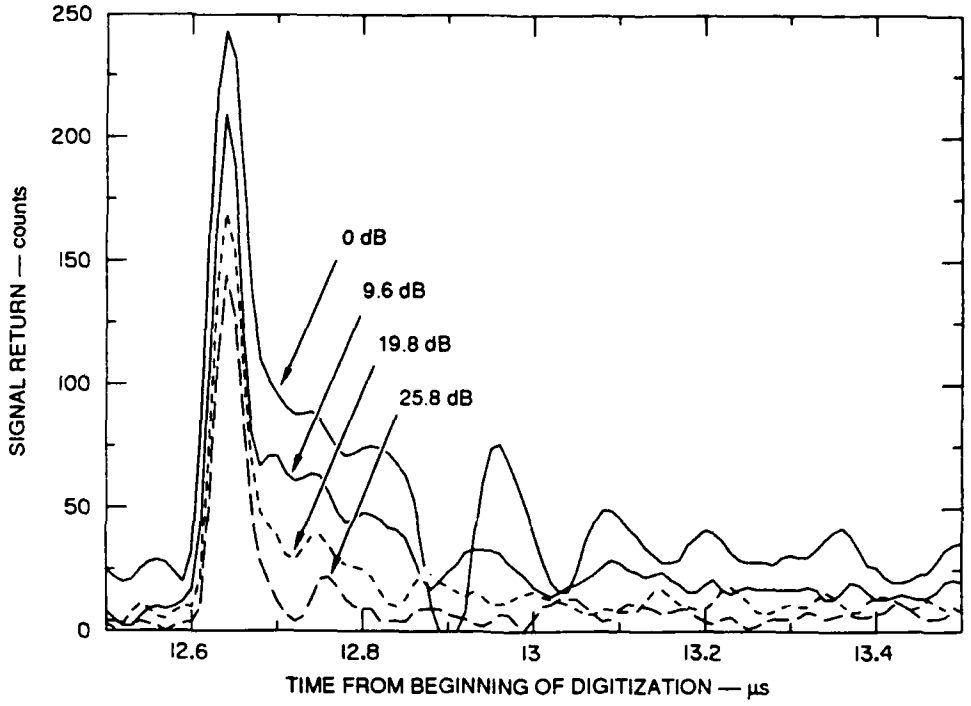

Figure 5-4. Representative multiwavelength lidar clear-air backscatter signatures before and after target (shown by peak) impaction. Traces are shown for one shot with no artificial attenuation, and also for shots acquired with the use of attenuating optical neutral density filters of 9.6, 19.8, and 25.8 dB, respectively.

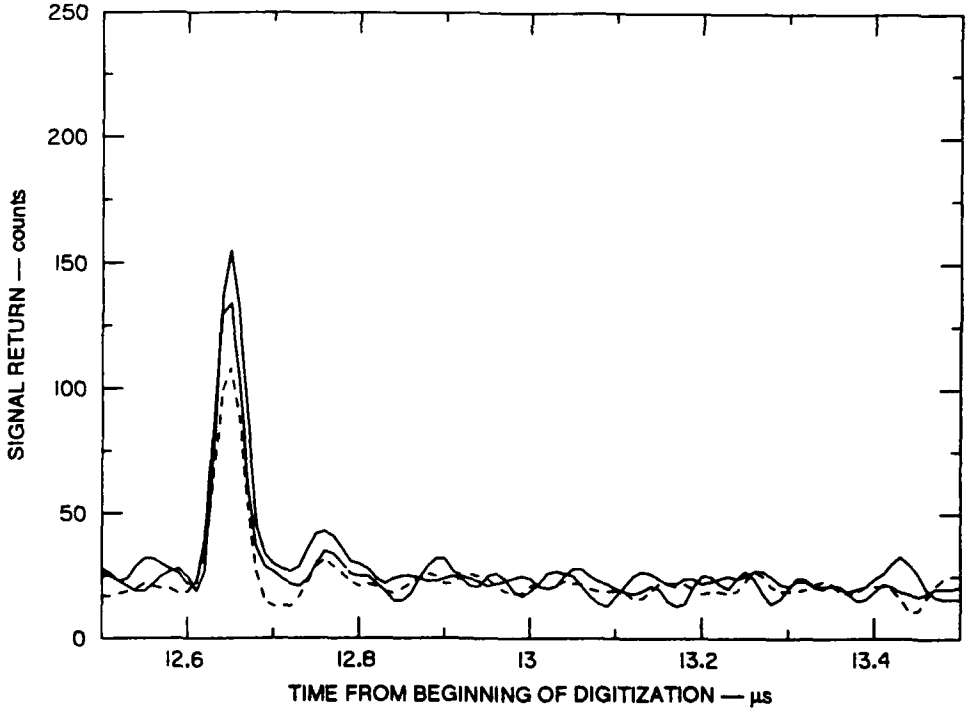

Figure 5-5. Multiwavelength lidar backscatter target returns for three consecutive shots taken through smoke, about 3 minutes after the calibration data presented in Figure 5-4.

6. LIDAR SIGNAL INVERSION MODEL

A computer model has been developed to simulate lidar system performance for attenuation of emitted laser energy by an intervening obscurant cloud, and to evaluate the sensitivity of the analytical two-lidar inversion technique to nonlinearities in logarithmic amplifier response. The model has the following modules. First, a model extinction profile is calculated from user input parameters using a simple square wave cloud or a Gaussian distribution function plus a background value. This profile is then combined with a user-defined constant or linearly varying range-dependent backscatter-to-extinction ratio to derive a corresponding backscatter profile. The backscattered power, P(r), received by the lidar from a volume of scatterers at range r is then calculated as

$$P(r) = \frac{K\beta(r)T^2(r)}{r^2}, \tag{6.1}$$

where K is a lidar system constant (arbitrary for modeling purposes), $\beta(r)$ is the atmospheric volume backscattering coefficient, and $T^2(r)$ is the two-way path transmittance

$$T^2(r) = \exp[-2\int_0^r \sigma(r')\ (1-f_{ms}(r'))\ dr'], \tag{6.2}$$

where $\sigma(r')$ is the volume extinction coefficient, and $f_{ms}(r')$ is an extinction correction factor between 0 and 1 that approximates the reduction in effective optical depth due to multiple scattering of photons into the laser beam along the direction of propagation. Kunkel and Weinman (1976) discussed the behavior of this extinction correction factor in detail. They used a Monte Carlo technique to derive mean values of this factor as a function of the optical penetration depth and receiver field of view. In particular, they found that, for receiver fields of view less than 10 mr, the mean factor $f_{ms}(r)$ is high for small optical depths but decreases rapidly with increasing optical depth, and then becomes nearly constant. For the sake of simplicity, in our model $f_{ms}(r)$ is assumed to vary linearly with penetration distance through the aerosol scattering obscurant.

The model backscattered power profile calculated from Equation (6.1) is then passed through a logarithmic amplifier function module, which simulates a nonlinear amplifier response by degrading the integrity of the backscattered signals. This is accomplished through application of one of the following operators to the backscatter signature at ranges beyond the peak backscatter signal: a running average, a

Gaussian distribution noise function, or a linearly decreasing rate of decay function. The resultant signals are corrected for the geometric range-squared effect, and then inverted to derive a calculated extinction profile using the analytical approach detailed in Section 4 (Equations 4.5 through 4.8). Derivatives are calculated using a 3-point central differencing scheme.

Figure 6-1 presents the results of an application of the simulation program to a two-lidar experiment where the lidars are separated by a distance of 1.9 km, and a Gaussian extinction model is assumed with a peak extinction of 4 km^{-1} at a range of 1.0 km from lidar 1. This extinction model corresponds to a total path transmission of about 35% (optical depth ~1). Other assumptions are a constant backscatter-to-extinction ratio, no degradation of the logarithmic amplifier response, and no multiple scattering. Plots are shown for the logarithmic backscatter power signature before and after correction for the range-squared effect, for the S-signal difference curve, and, finally, for the model and retrieved extinction profiles. As expected, the inversion correctly retrieves the input extinction model.

The linearized, range-corrected power signatures, S(r), presented in Figure 6-1b differ significantly from the analogous signatures shown in Figures 4-11 to 4-13 for actual smoke measurements. Whereas the modeled returns for either lidar are markedly lower on the far side of the smoke cloud than the near side, due to attenuation through the cloud, the actual measured returns are approximately equal on both sides of the cloud. Of course, the magnitude of the expected difference between the signals on the near and far sides of the cloud is a function of the optical depth of the cloud, but the difference in optical depths between the model and observed clouds cannot explain the observed behavior, as it is characteristic of measurements (not shown) obtained through smokes with optical depths equivalent to or greater than the model optical depth. This behavior is probably a combination of two effects: the lower limit of signal decay imposed by the background noise threshold of the lidar systems, and the response characteristics of the logarithmic amplifiers. The latter deserves some elaboration. As noted in Section 5, each amplifier has a characteristic, finite decay response time. For measurements taken through an obscurant cloud that is composed of inhomogeneously distributed density elements -- that is, a superposition of extinction minima and maxima -- the measured backscatter signature itself becomes a superposition of signals that appear to overestimate the true backscattered radiation from the aerosols due to the slow recovery time of the logarithmic amplifier. Within the smoke cloud, this behavior apparently has grave consequences for the inversion of the measurements using the analytical two-lidar method. At ranges on the far side of the cloud, the amplifier response may have a cumulative effect that results in an artificially elevated signal level.

Figure 6-2 presents results for the same case shown in Figure 6-1, except the lidar signals received from ranges beyond the peak of the backscattered lidar signal have been passed through a 21-point running average filter. The resultant S-difference curve departs significantly from the "true" difference curve shown in Figure 6-1, and the inversion yields incorrect extinction values within the region defined

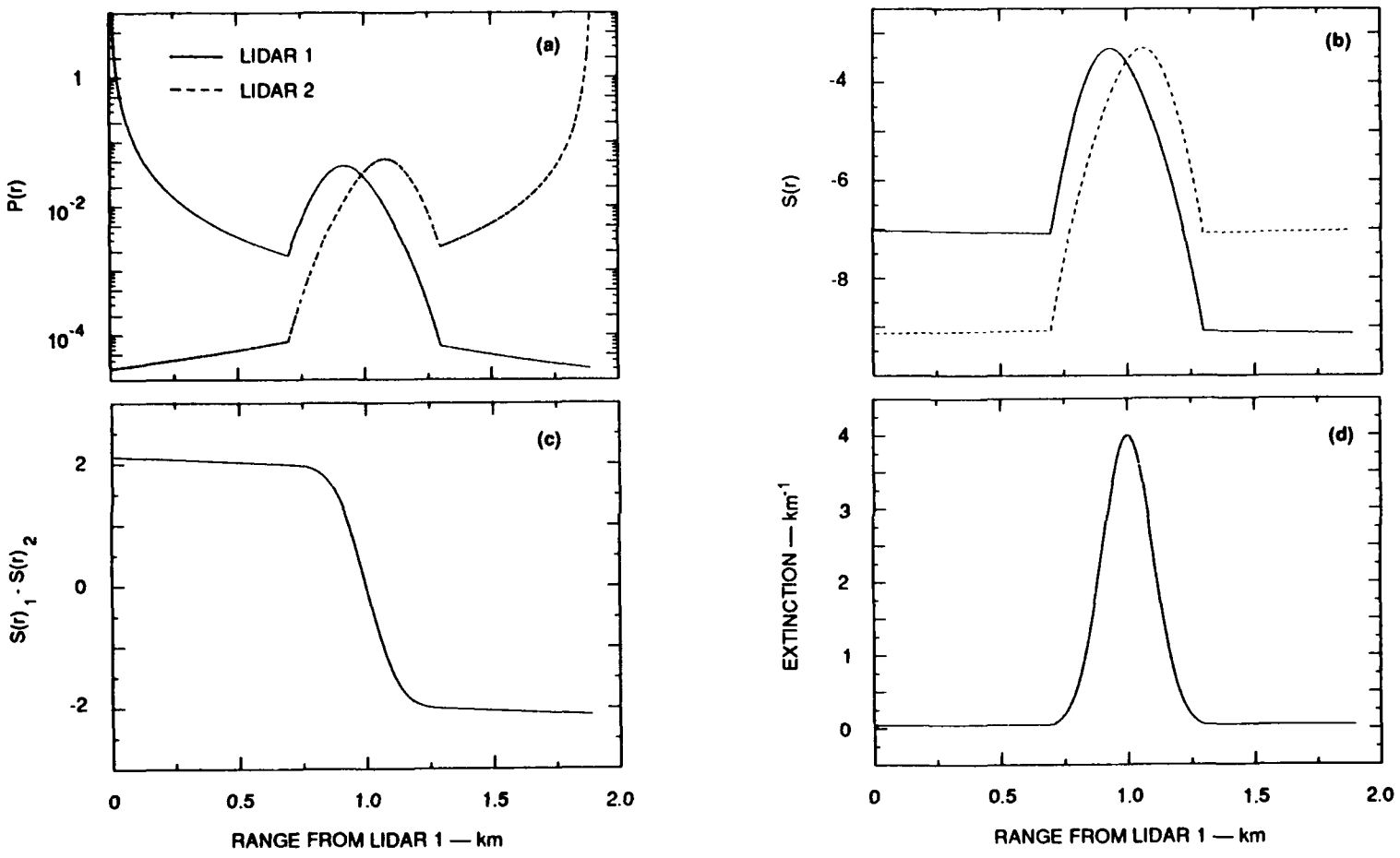

Figure 6-1. Application of the two-lidar analytical inversion technique to simulated lidar measurements of a Gaussian extinction model with a peak extinction of 4 km^{-1}, with no degradation of logarithmic amplifier response and no multiple scattering: (a) logarithmic backscattered power signatures before removal of geometric range dependence, (b) same signatures after correction for geometric range dependence, (c) signal differences, and (d) model and retrieved extinction profiles.

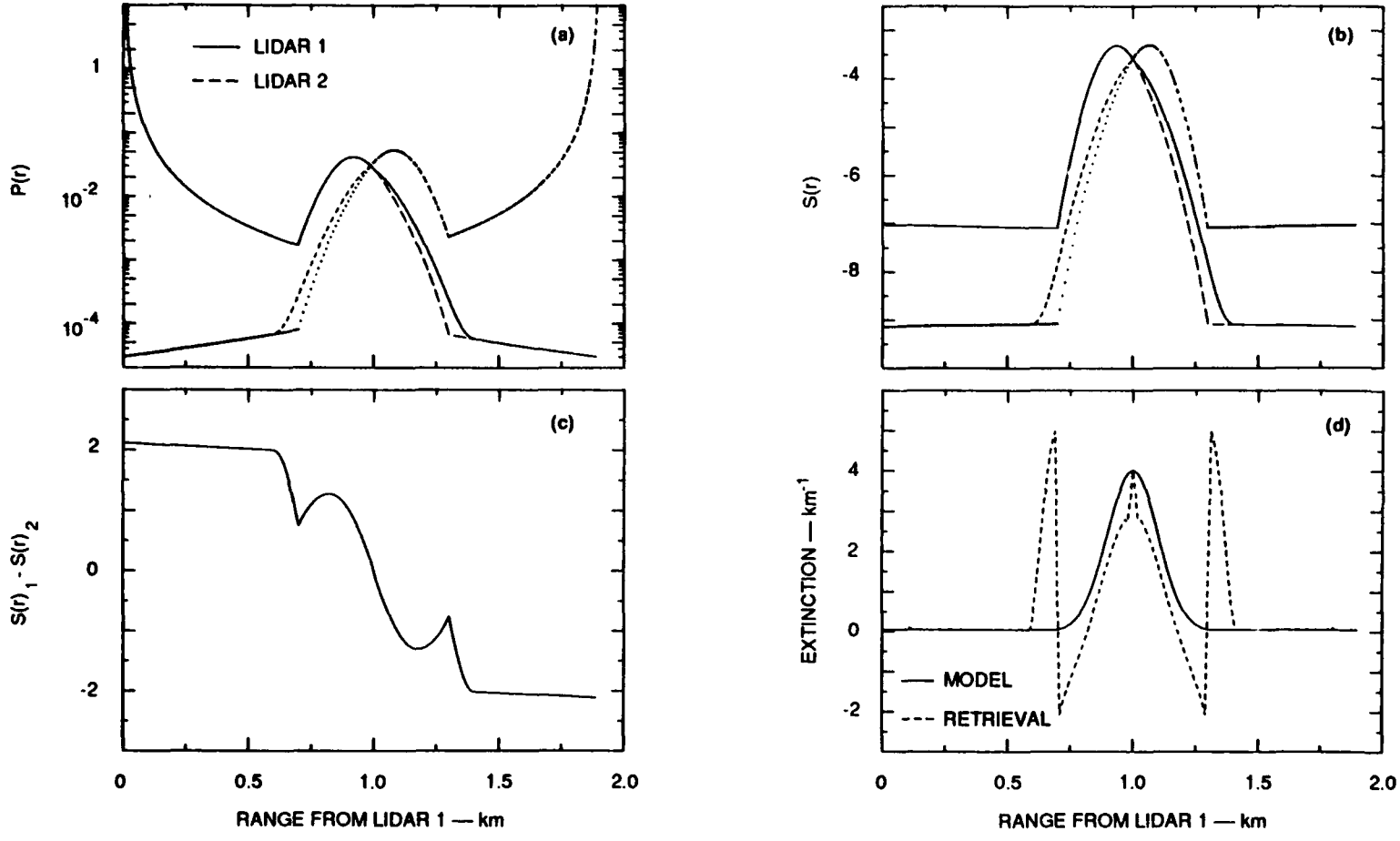

Figure 6-2. Results for same case presented in Figure 6-1, except where received lidar signals at ranges beyond the peak of the backscattered lidar signal have been degraded by passing them through a 21-point running average filter.

by the Gaussian extinction model, except near the peak. The peak backscattered signal does not coincide with the model backscatter profile peak because of the transmittance term. It should be noted that the 21-point running average utilized in the logarithmic amplifier module introduces noise into the backscattered signals only at those ranges that are at least 10 bins beyond (with respect to each lidar) the peak of the Gaussian extinction distribution. This may account for the good agreement between the retrieval and the model at the peak, and the physically realistic underestimates near the peak.

Figure 6-3 presents results for a similar case where the signals have been degraded by linearly decreasing rates of decay that differ for each lidar system. In particular, at ranges beyond the peak backscattered signal (before range correction), the power at range r_{j+1} (where $r_{j+1} > r_j$ with respect to each lidar) is calculated as

$$P(r_{j+1}) = P(r_{j+1}) + f_{drop}*[P(r_j)-P(r_{j+1})], \tag{6.3}$$

where f_{drop} is input by the user and represents the fractional amount of the power between signals at adjacent ranges by which the signal at the greater range from the lidar will be increased. In this example, f_{drop} equals 0.7 for lidar 1 and 0.6 for lidar 2, so lidar 1 experiences a more slowly decreasing rate of decay than lidar 2. Not surprisingly, the curve for the signal differences is quite similar to the corresponding curve for the previous case (running average), and the resultant extinction retrieval is similarly poor.

Finally, the results of a simulation run with multiple scattering are presented in Figure 6-4. In this example, a Gaussian extinction model with a peak extinction value of 10 km^{-1} is assumed, and a maximum multiple scattering factor, $f_{ms}(r)$, of 0.5 is used. The optical depth along the path is shown with and without the multiple scattering term for each lidar to demonstrate the increase in transmission (decrease in optical depth) that results. The effect on the inversion of including the multiple scattering factor is merely to reduce the magnitudes of the retrieved extinction coefficients. This has no effect on the general shape of the retrieved extinction profile because the simple multiple scattering correction affects the transmittance term only. In practice, the presence of multiply scattered light would be expected to widen the pulse, as discussed in Section 5. This effect has not been included in the simple model presented here.

In conclusion, the results of simulations performed with a relatively simple lidar system performance model have shown that small nonlinear perturbations in the response of a logarithmic amplifier, similar to those observed in the SRI systems used in the CECATS test, can lead to gross errors in retrieved extinction profiles derived using the analytical two-lidar inversion technique. These results are observed

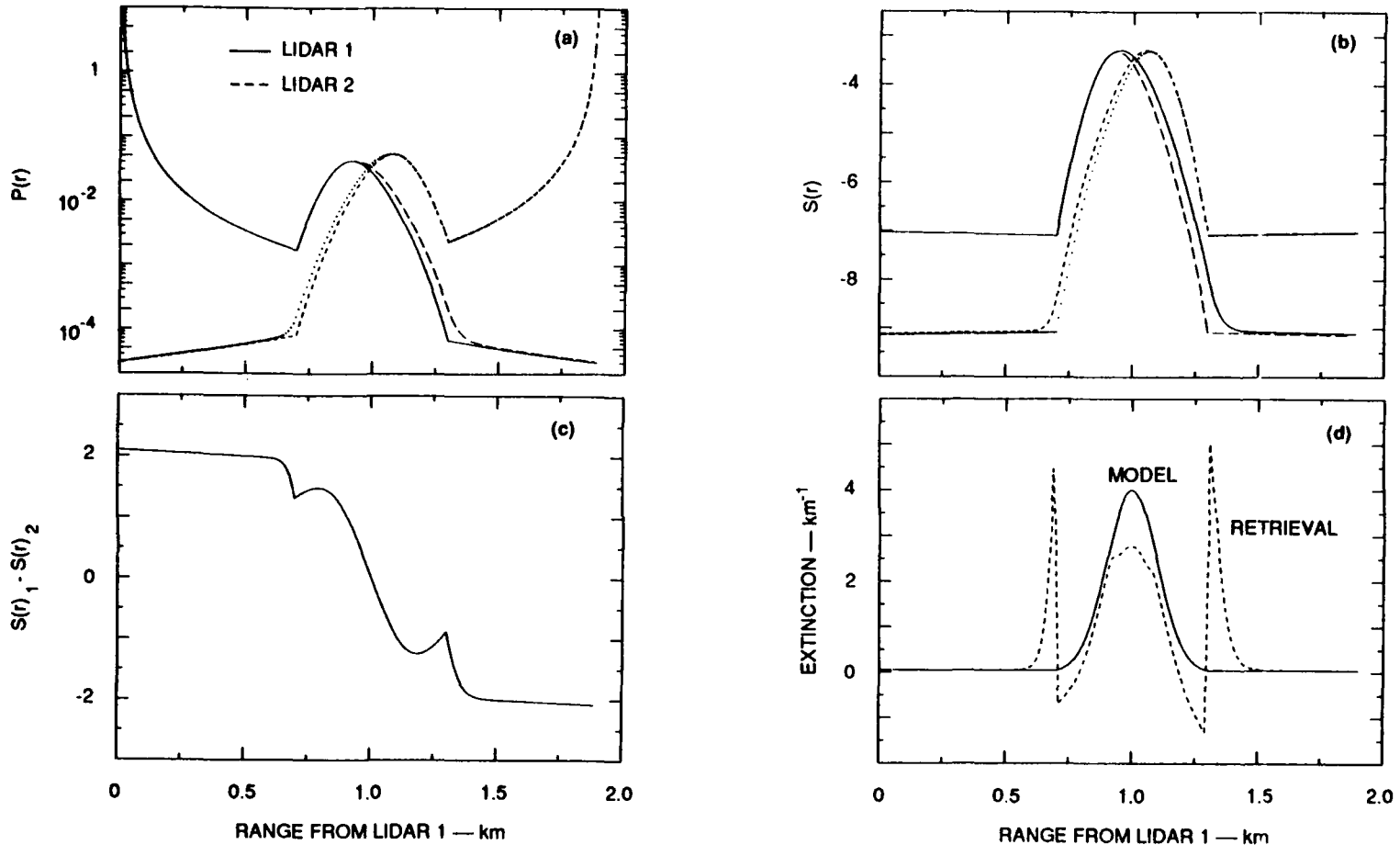

Figure 6-3. Results for same case presented in Figure 6-1, except where signals have been degraded by application of linearly decreasing rates of decay that differ for each lidar.

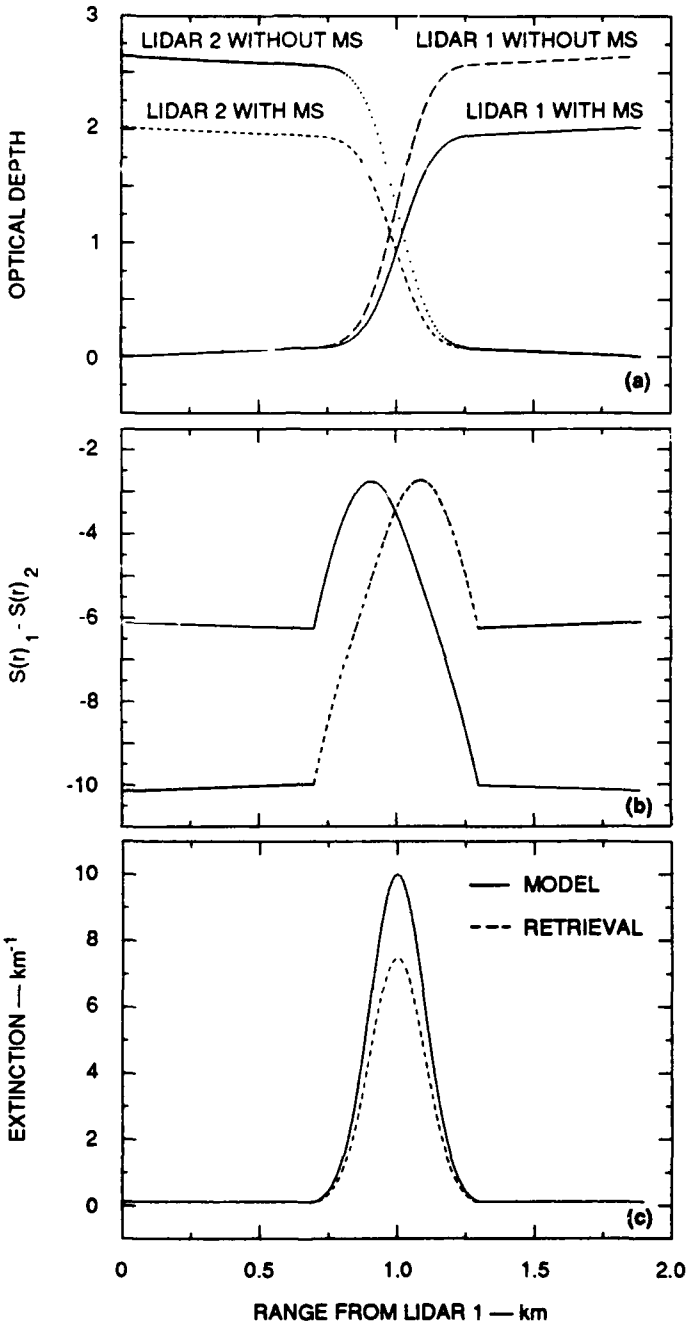

Figure 6-4. Application of the two-lidar analytical inversion technique to simulated lidar measurements of a Gaussian extinction model with a peak extinction of 10 km^{-1}, where multiple scattering of the transmitted beams has been taken into account: (a) range-dependent optical depth with and without inclusion of multiple scattering correction, (b) signal differences, and (c) model and retrieved extinction profiles.

in the absence of any other sources of noise in the backscattered signals. It is important to note that in the simulations that have been performed here, the extinction model (and resulting backscatter model) has been assumed to be a monomodal Gaussian distribution, which represents an enormous oversimplification of the distribution of particulates in real atmospheric smoke plumes, in which the scatterers are neither monomodally nor uniformly distributed. In fact, the backscatter signatures that we have measured through smoke obscurants are characterized by a superposition of several signal maxima, which, when operated on by a nonlinearly responding logarithmic amplifier, can only complicate the inversion process.

7. CONCLUSIONS AND RECOMMENDATIONS

A unique two-lidar experiment was conducted as part of the CECATS tests. The data were used to again illustrate the problems of single-lidar analysis technique for deriving optical density profiles through dense obscurant events. The two-lidar technique should provide a method of evaluating optical density profiles without the uncertain assumptions needed by the single-lidar analysis techniques. However, the two-lidar analysis method applied to the CECATS lidar data did not provide satisfactory data on obscurant density distributions. By analyzing collected data in terms of lidar response functions and by conducting a modeling study of the two-lidar analysis method, it is concluded that small nonlinear perturbations in the lidar logarithmic response and signal amplifier recovery times following observation of strong lidar returns can lead to large errors in two-lidar retrievals of optical density profiles. Improvement of the performance of the logarithmic amplifiers used in the SRI lidar systems is needed before they can be used to evaluate the performance of the two-lidar technique for determination of range-resolved obscurant densities.

ACKNOWLEDGMENTS

The authors thank Walter A. Flood of the Geosciences Division of the U.S. Army Research Office (ARO) and Anthony Van de Wal of the Office of the Project Manager Smokes/Obscurants (PM Smoke) for their support. The lidars were operated by Norman B. Nielsen and Louis J. Salas. Bruce M. Morley assembled the data systems.

REFERENCES

Evans, B., Paper presented at AGARD Electromagnetic Propagation Conference, Copenhagen, Denmark, 1989.

Farmer, W.M., B.A. Locke, R.F. Soto, R.E. Davis, J.E. Steedman, and R. Laughman, "Characterization, evaluation, and comparison of army transmissometer systems (CECHTS). Quick-Look Report 37, Science and Technology Corporation, Hampton, VA 23666, 1988.

Fernald, F.G., B.M. Herman, and J.A. Reagon, "Determination of aerosol height distributions by lidar," *J. Appl. Meteor.*, 1972, Vol. 11, pp. 482-489.

Hughes, H.G., and M.R. Paulson, "Double-ended lidar technique for aerosol studies," *Appl. Opt.*, 1988, Vol. 27, pp. 2273-2278.

Klett, J.D., "Stable analytical inversion solution for processing lidar returns," *Appl. Opt.*, 1981, Vol. 20, pp. 211-220.

Kunkel, K.E., and J.A. Weinman, "Monte Carlo analysis of multiply scattered lidar returns," *J. Atmos. Sci.*, 1976, Vol. 33, pp. 1772-1781.

Kunz, G.J., "Bipath method as a way to measure the spatial backscatter and extinction coefficients with lidar," *Appl. Opt.*, 1987, Vol. 26, pp. 794-795.

Uthe, E.E., "Lidar evaluation of smoke and dust clouds," *Appl. Opt.*, 1981, Vol. 20, pp. 1503-1510.

Uthe, E.E., "Application of surface based and airborne lidar system for environmental monitoring," *APCA Journal*, 1983, Vol. 33, pp. 1149-1155.

Uthe, E.E., and J.M. Livingston, "Lidar extinction methods applied to observations of obscurant events," *Appl. Opt.*, 1986, Vol. 25, pp. 38-44.